January 19, 2007

MEMORANDUM TO: Thomas Martin, Director
Division of Safety Systems
Office of Nuclear Reactor Regulation

FROM: Ralph Landry, Acting Chief **/RA/**
Nuclear Performance and Code Review Branch
Division of Safety Systems
Office of Nuclear Reactor Regulation

SUBJECT: TECHNICAL AND REGULATORY BASIS FOR THE REACTIVITY-INITIATED ACCIDENT INTERIM ACCEPTANCE CRITERIA AND GUIDANCE

The Nuclear Performance and Code Review Branch (SNPB) developed the enclosed technical and regulatory basis document for the reactivity-initiated accident (RIA) interim acceptance criteria and revised guidance. This document identifies deficiencies in certain regulatory guidance documents (RG 1.77, 1.183, and 1.195) and defines interim acceptance criteria and revised guidance (related to fission-product gap inventory) for the RIAs. This document provides the basis for an upcoming revision to the NUREG-0800, Standard Review Plan, Section 4.2, Fuel System Design. The development of the interim acceptance criteria builds upon a safety assessment of currently operating plants documented in Research Information Letter 0401, dated March 31, 2004. The basis for the interim acceptance criteria and revised guidance has been discussed with the industry during two public workshops on November 9, 2006 and December 19, 2006.

CONTACT:
Paul M. Clifford, NRR/DSS/SNPB

Attachment: As stated

Distribution: JWermiel RLandry PClifford

ACCESSION NUMBER: ML070220400

DSS/SNPB	DSS/SNPB
PCLIFFORD	RLANDRY
1/18/07	1/18/07

C:\FileNet\ML070220400.wpd

ATTACHMENT

TECHNICAL AND REGULATORY BASIS: INTERIM ACCEPTANCE CRITERIA AND GUIDANCE FOR THE REACTIVITY-INITIATED ACCIDENT

1.0 INTRODUCTION

The purpose of this report is to document the technical and regulatory basis of the interim acceptance criteria and guidance for the reactivity-initiated accident (RIA). RIAs consist of postulated accidents which involve a sudden and rapid insertion of positive reactivity. These accident scenarios include a control rod ejection (CRE) for pressurized water reactors (PWRs) and a control rod drop accident (CRDA) for boiling water reactors (BWRs).

As illustrated in Figure 1-1, the uncontrolled movement of a single control rod out of the core results in a positive reactivity insertion which promptly increases local core power. Fuel temperatures rapidly increase prompting fuel pellet thermal expansion. The reactivity excursion is initially mitigated by Doppler feedback and delayed neutron effects followed by reactor trip. Standard Review Plan (SRP) Section 15.4.8 and 15.4.9 provide further detail on the CRE and CRDA respectively.

Figure 1-1: Fuel Response to a Rapid Reactivity Insertion

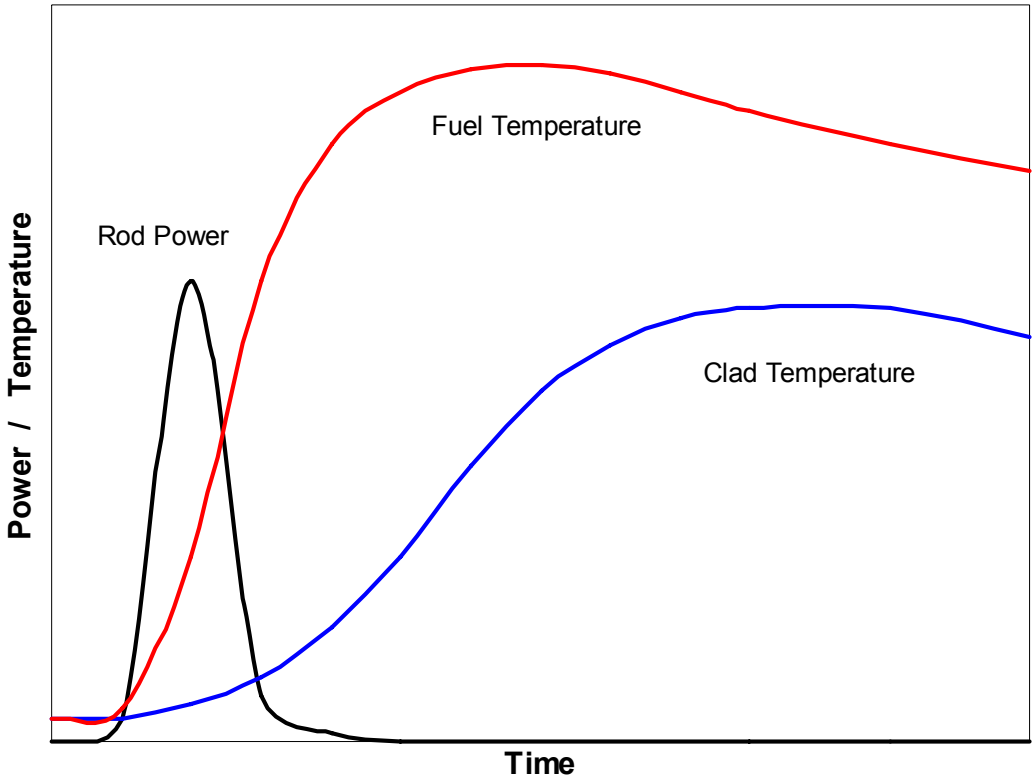

2.0 REGULATORY EVALUATION

10CFR50 Appendix A, General Design Criterion 28 (GDC28) requires the reactivity control system to be designed with appropriate limits on the potential amount and rate of reactivity increase to assure that the effects of postulated reactivity accidents can neither:

a. Result in damage to the reactor coolant pressure boundary greater than limited local yielding, nor

b. sufficiently impair core cooling capability.

Because the PWR rod ejection and BWR rod drop accidents are classified as Condition IV events, fuel rod failure may occur during these events - provided offsite and control room radiological consequences remain within acceptable limits. Specific guidance on the implementation of GDC28 requirements have been detailed within Regulatory Guide (RG) 1.77 and NUREG-0800 Standard Review Plan. RG 1.77 identifies acceptable PWR analytical methods and assumptions as well as the following acceptance criteria to address GDC 28.

1. Fuel radial average energy density limited to 280 cal/g at any axial node.
2. Maximum reactor pressure limited to the value that will cause stresses to exceed Service Level C as defined in the ASME Boiler and Pressure Vessel code.
3. Offsite dose consequences limited to "well within" the guidelines in 10CFR Part 100.

The basis of the first criteria on fuel enthalpy is to maintain a coolable geometry. **As discussed in Section 3, the current RG 1.77 criterion of 280 cal/g has been judged inadequate to ensure fuel rod geometry and long-term coolability are maintained**.

The basis of the second criteria on reactor pressure is to maintain the integrity of the reactor pressure boundary. Service Level C is adequate to satisfy this basis. Note that the calculation of peak pressure must include (1) any RCS pressure increase associated with the core power excursion and (2) any mechanical energy generated from fuel-coolant interaction (FCI). **Potential contributions from FCI have not been properly addressed.**

The basis of the third criteria on offsite dose is to protect the health and safety of the public. This criterion, by itself, is adequate and not being altered. Note that the total fission product inventory available for release must include (1) steady-state fuel/clad gap fraction and (2) transient-induced gas release from the fuel pellet. **Contributions to the total radiological source term from transient-induced gas release have not been properly addressed in current regulatory guidance (RG 1.183 and 1.195).**

RG 1.77 states that the number of fuel rods experiencing clad failure should be calculated and used to obtain the amount of contained fission product inventory released to the reactor coolant system. NUREG-0800 Standard Review Plan Section 4.2 defines RIA fuel clad failure criteria.

1. Radial average fuel enthalpy greater than 170 cal/g for BWRs at zero or low power,
2. Local heat flux exceeding fuel thermal design limits (e.g. DNBR and CPR) for all PWR events and at-power events in BWRs.

The 170 cal/g criterion is not always adequate to protect fuel rod integrity.

3.0 TECHNICAL EVALUATION

For many years, the NRC was aware of potential problems with the RIA acceptance criteria (See Section 2.0). In 1980, MacDonald et al. (Reference 1) reviewed earlier test data from SPERT and TREAT (which form the basis of the current regulatory limits) and then compared these earlier tests to the then recent PBF test results. MacDonald concludes that:

1. The NRC expressed the RIA criteria in terms of fuel enthalpy, whereas the SPERT and TREAT data were reported in terms of total energy deposition. Based on this difference, a more appropriate value for the RIA criteria would have been 230 cal/g.
2. LWR fuel rods subjected to the regulatory limit, radial average fuel enthalpy of 280 cal/g, will be severely damaged and post-accident cooling may be impaired.
3. PCMI clad failure may result at a radial average fuel enthalpy of 140 cal/g on irradiated LWR fuel rods as compared to the 170 cal/g failure criteria.
4. Fuel grain-boundary separation and powdering also contribute to a loss of rod geometry during quenching.
5. The mode of fuel rod failure is strongly dependent on previous irradiation history.

Based upon calculated peak fuel enthalpy using best-estimate methods, with the effects of void formation and prompt moderator feedback included, MacDonald et al. concludes that no real safety concern exists.

In response to the latest results from international RIA test programs (e.g. NSRR, CABRI, IGR, and BIGR), the NRC completed an assessment of currently operating reactor. Research Information Letter 0401 (Reference 2) compiled all of the RIA test results and performed limited scaling to account for non-prototypical test conditions. Figures 3.0-1 through 3.0-5 present an expanded compilation of RIA test results originally documented within RIL 0401. Figures 3.0-6 and 3.0-7 present the scaled, adjusted fuel enthalpy results for the same expanded compilation. Note that these figures also include five more recent NSRR test results (20 °C, 0.1 MPa, 4.4 ms pulse):

(1) VA-1, MDA cladding, 78 GWd/MTU, 73 microns of oxide - failed at 61 cal/g

(2) VA-2, ZIRLO cladding, 79 GWd/MTU, 70 microns of oxide - failed at 55 cal/g.

(3) OI-12, MDA cladding, 39 GWd/MTU, 15 microns of oxide, 108 cal/g - no failure reported.

(4) RH-1, M5 cladding, 67 GWd/MTU, 10 microns of oxide, 127 cal/g - no failure reported.

(5) MR-1, Zr-4 cladding, 71 GWd/MTU, 39 microns of oxide, 89 cal/g - no failure reported.

As part of RIL 0401, best-estimate neutronics analyses were performed for a range of LWR conditions and it was found that the control rod worth needed to reach the cladding failure threshold were beyond expected values. Without cladding failure, coolable geometry is ensured and energetic fuel-to-coolant interaction is avoided. This regulatory position is similar to that of MacDonald 20+ years earlier.

Figure 3.0-1: RIA Empirical Results - Peak Fuel Enthalpy versus Burnup

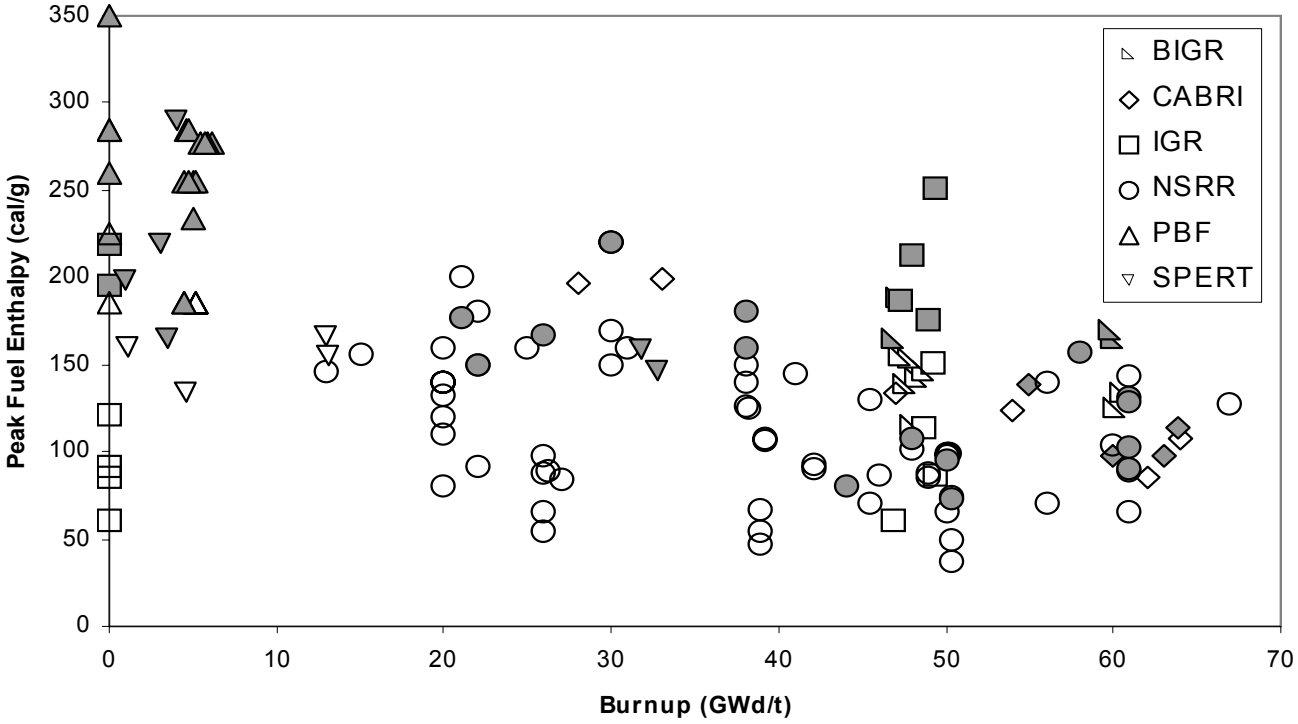

Figure 3.0-2: RIA Empirical Results - Peak Fuel Enthalpy versus Pulse Width

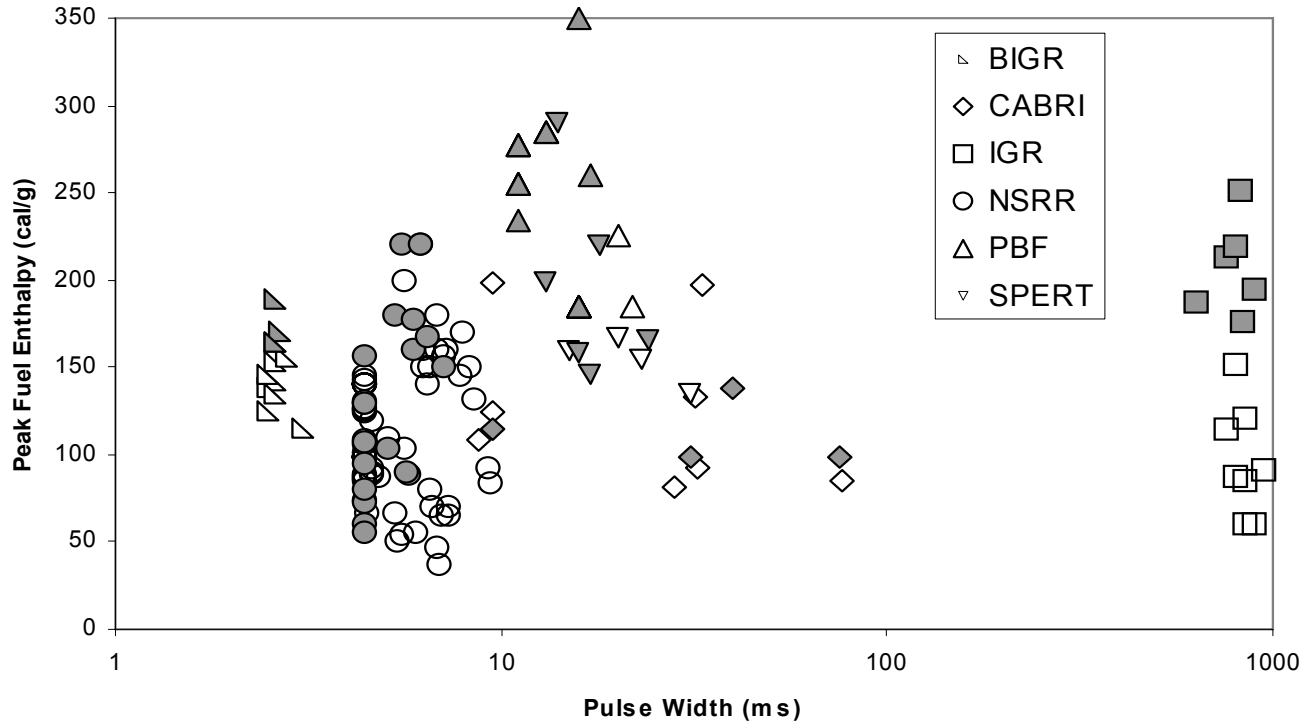

Figure 3.0-3: RIA Empirical Results - Fuel Enthalpy Rise versus Burnup

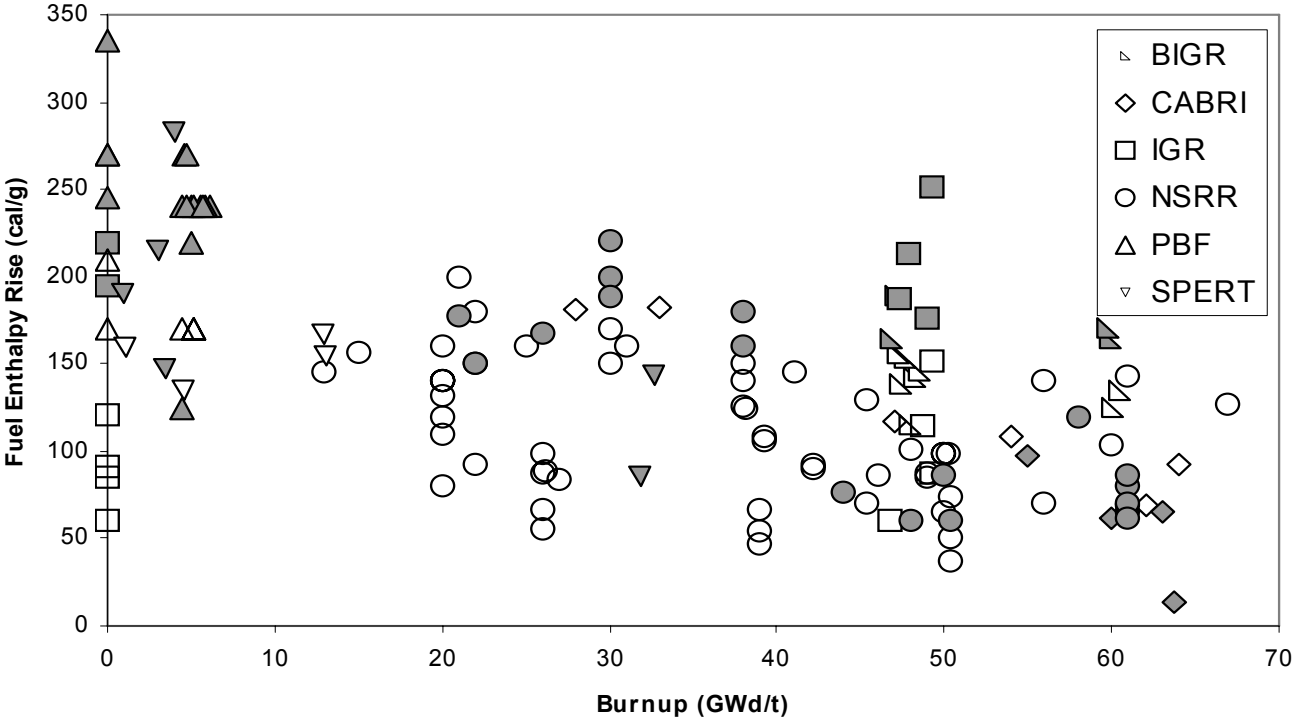

Figure 3.0-4: RIA Empirical Results - Fuel Enthalpy Rise versus Oxide/Cladding Ratio

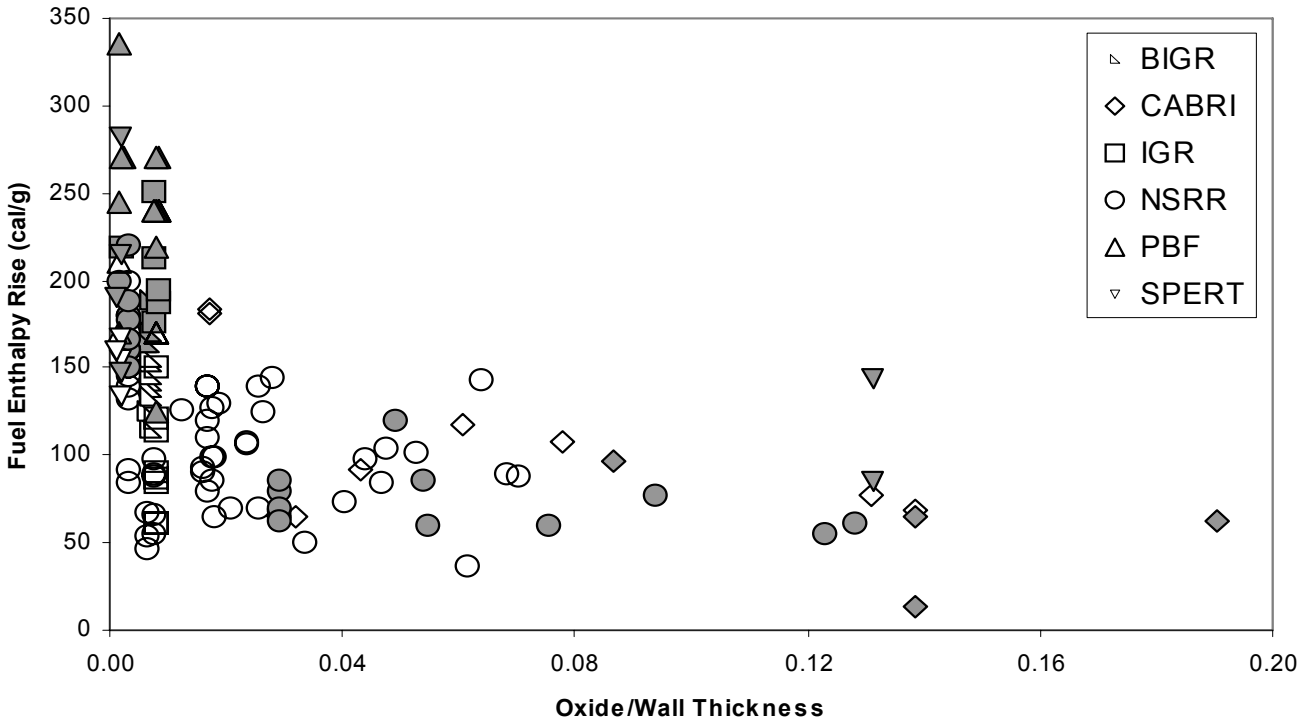

Figure 3.0-5: RIA Empirical Results - Fuel Enthalpy Rise versus Oxide Thickness

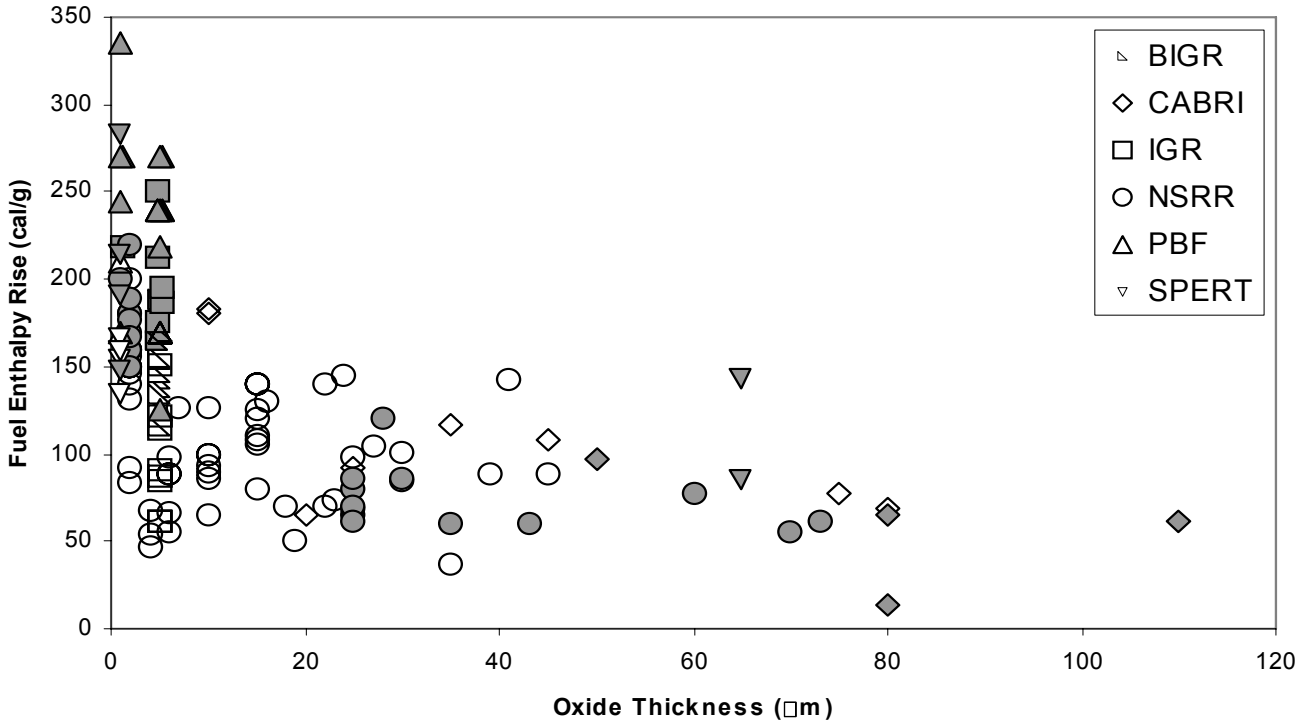

Figure 3.0-6: RIL 0401 Adjusted Fuel Enthalpy Rise versus Oxide Thickness

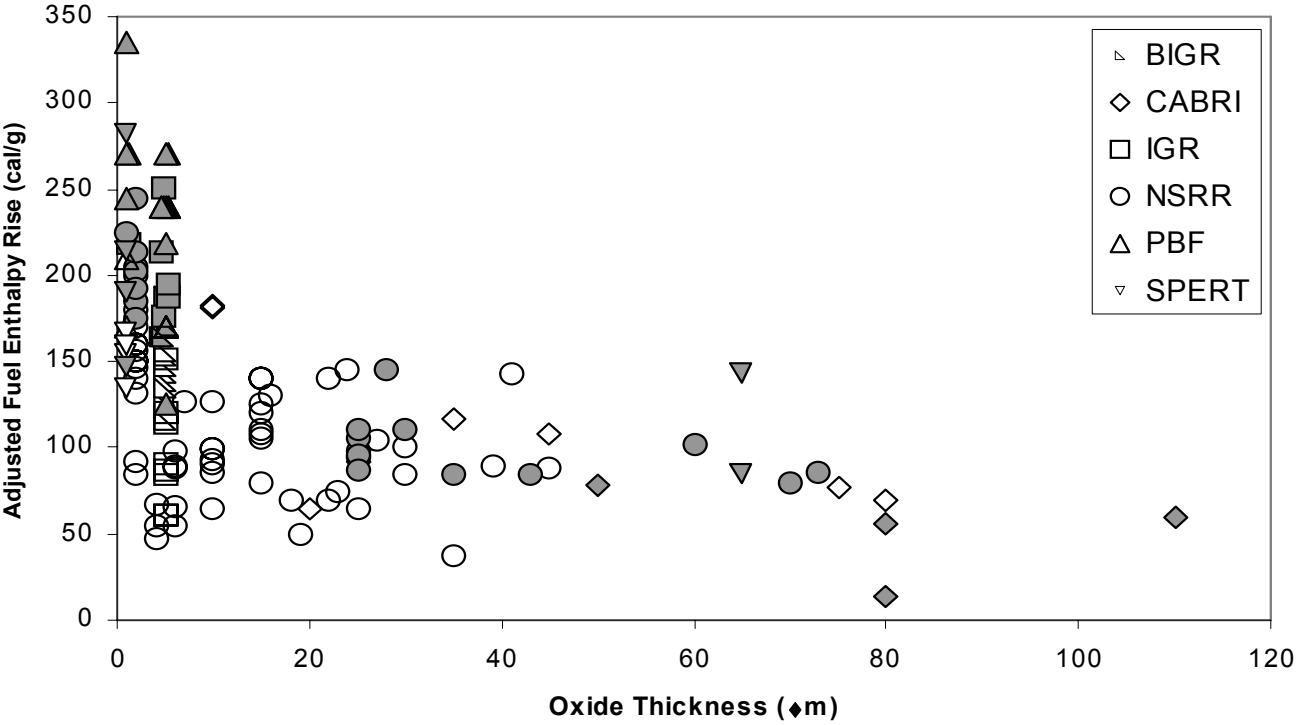

Figure 3.0-7: RIL 0401 Adjusted Fuel Enthalpy Rise versus Oxide/Wall Thickness

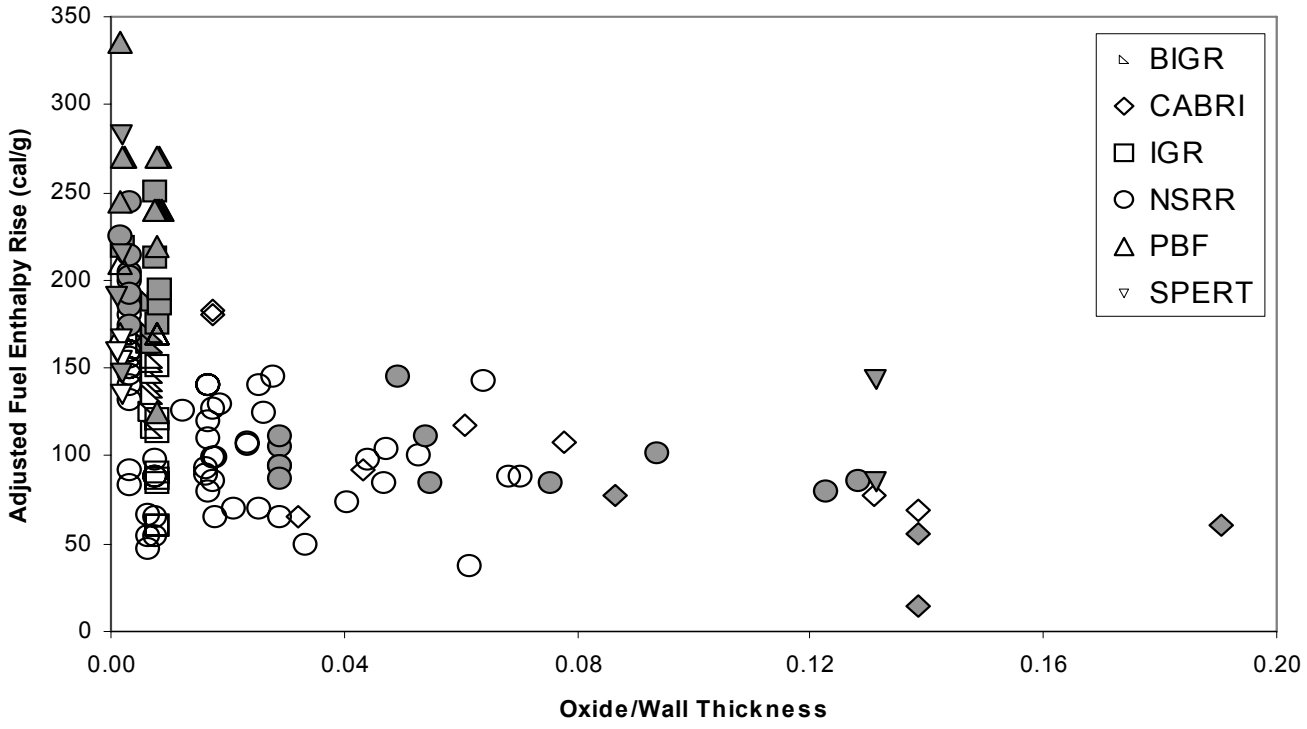

3.1 Fuel Cladding Failure Criteria

The number of fuel rod failures must not be underestimated in order to ensure a conservative dose calculation. Fuel cladding failure mechanisms associated with RIAs include:

1. Pellet-to-cladding mechanical interaction (PCMI) high-strain-rate cladding failure.
2. Fission product-induced swelling of molten fuel.
3. High-temperature cladding plastic deformation.
4. Post-DNB cladding oxidation and embrittlement and high-temperature creep.

MacDonald et al. concluded that the mode of fuel rod failure is strongly dependent on previous irradiation history. Irradiation history would include power history, burnup, and in-service cladding corrosion (oxidation). Other important factors contributing to fuel rod failure include (1) the initial conditions of the fuel rod (e.g. initial fuel enthalpy, fuel-to-clad gap, rod internal pressure), (2) the initial conditions of the reactor coolant (e.g. temperature, pressure, mass flow), and (3) fuel design. Of course, the governing influence on the fuel rod's response to the postulated transient is the amount and rate of reactivity insertion. The influence of each of these factors differs for each failure mechanism.

Failure mechanisms #1 and #4 are discussed in more detail below in Section 3.1.2. Failure mechanisms #2 and #3 are avoided by precluding incipient fuel melting (See Section 3.2.1) and will not be further discussed.

3.1.1 Interim Criteria

Based upon an assessment of the RIA empirical database and building upon RIL 0401, the following fuel cladding failure criteria are proposed.

1. **The high cladding temperature failure criteria for zero power conditions is a peak radial average fuel enthalpy greater than 170 cal/g for fuel rods with an internal rod pressure at or below system pressure and 150 cal/g for fuel rods with an internal rod pressure exceeding system pressure. For intermediate and full power conditions, fuel cladding failure is presumed if local heat flux exceeds thermal design limits (e.g. DNBR and CPR).**
2. **The PCMI failure criteria is a change in radial average fuel enthalpy greater than the corrosion-dependent limit depicted in Figure 3.1-3 (PWR) and Figure 3.1-9 (BWR).**

The total number of fuel rods which must be considered in the radiological assessment is equal to the summation of all of the fuel rods failing each of the criteria. Applicants do not need to double count fuel rods which are predicted to fail more than one of the criteria.

3.1.2 Technical Basis

The following section describes the basis of the fuel cladding failure criteria. Fuel cladding failure may occur almost instantaneously during the prompt fuel enthalpy rise (due to PCMI) or may occur as total fuel enthalpy (prompt + delayed), heat flux, and cladding temperature increase. For the purpose of calculating fuel enthalpy for assessing PCMI failures, the prompt fuel enthalpy rise is defined as the radial average fuel enthalpy rise at the time corresponding to one pulse width after the peak of the prompt pulse. For assessing high cladding temperature failures, the total radial average fuel enthalpy (prompt + delayed) should be used.

High Cladding Temperature Failure:

Fuel rod cladding with low corrosion levels (i.e. minimal hydrides) maintains sufficient ductility to absorb a relatively large amount of cladding strain resulting from fuel pellet thermal expansion. As a result, PCMI failure will be less limiting than non-PCMI failure mechanisms. High cladding temperature failure mechanisms have been observed at many of the test programs. Based upon reported fuel failure test results at IGR and BIGR, RIL 0401 (Reference 2) noted that the traditional 170 cal/g (total radial average fuel enthalpy) remains an acceptable failure threshold. The following discussion will propose a more conservative criteria for fuel rods with an internal pressure exceeding system pressure.

High temperature cladding failures are sensitive to factors which influence fuel-to-clad-to-coolant heat transfer, factors which influence rod internal pressure, and total fuel enthalpy. Whereas, PCMI is more sensitive to factors which influence fuel thermal expansion and cladding material properties.

Figure 3.1-1 provides a closer look at the RIA empirical database from Section 3.0 - excluding PCMI failure and high fuel enthalpy PBF test results. The proposed high cladding temperature failure criteria, 170 cal/g (peak radial average fuel enthalpy), is included on this figure. Three of the high burnup BIGR failed specimens fall just below the proposed criteria. In addition, several earlier, zero burnup NSRR test results (not included in the RIA database discussed in Section 3.0) exhibited non-PCMI, high cladding temperature failure below the proposed 170 cal/g (total radial average fuel enthalpy). Figure 3.1-2 provides an expanded database of non-PCMI failures as a function of cladding differential pressure (including earlier NSRR tests). Note that this figure was provided by EPRI during a public workshop. Examination of this figure reveals that non-PCMI cladding failures, including high temperature cladding creep (balloon/burst), were reported below 170 cal/g when rod internal pressure exceeded the pressure within the experimental capsule. To account for this differential pressure dependant failure mechanism, a second high cladding temperature failure criteria of 150 cal/g is proposed for fuel rods with an internal pressure in excess of reactor system pressure.

For the purpose of calculating peak fuel enthalpy for both cold and hot conditions, zero fuel enthalpy is defined at 20 °C (68 °F).

As described below in Table 3.1-1, the RIA database encompasses a wide array of fuel rod designs, cladding alloys, and experimental conditions (e.g. pulse width, temperature, etc.). Fuel specimens were fabricated from BWR, PWR, and VVER commercial rods and research reactor fuel rods and included cladding alloys: Zr-2, Zr-4, low tin Zr-4, ZIRLO, M5, E110, and MDA. Based upon this comprehensive database, it is judged that the proposed non-PCMI, high cladding

temperature fuel cladding failure criteria conservatively predict cladding failure (e.g. balloon/burst, post-DNB oxidation/embrittlement) at zero power conditions for both BWRs and PWRs. However, since the database does not encompass all power operating conditions (e.g. coolant conditions, DNB thermal margins, etc.), fuel rods operating at-power conditions (≥ 5% rated thermal power) which are predicted to exceed thermal design limits (DNB and CPR) must be assumed to fail and must be accounted for in the dose calculation.

Table 3.1-1: RIA Empirical Database

Parameter	Minimum	Maximum
Cladding O.D. (mm)	7.92	14.5
Wall Thickness (μm)	495	915
Oxide Thickness (μm)	0	110
Oxide/Wall Ratio	0.001	0.19
Fuel Rod Burnup (GWd/MTU)	0	79
Pulse Width (msec)	2.5	950
Deposited Energy (cal/g)	51	695
Peak Fuel Enthalpy (cal/g)	37	350
Fuel Enthalpy Rise (cal/g)	14	335

PWR Fuel PCMI Failure:

Based upon an assessment of the empirical data, RIL 0401 established that PCMI cladding failure is more dependent on initial cladding oxidation than on burnup. It is important to recognize that cladding hydrogen concentration is a key factor in the cladding failure process and that cladding oxidation is used as a surrogate for hydrogen concentration.

After scaling portions of the empirical data (failed rods only) to account for non-prototypical test conditions (See Figure 3.0-6), RIL 0401 developed a lower-bound fuel failure threshold (Figure 21 of Reference 2). The RIL 0401 failure threshold starts at 150 Δcal/g (change in fuel enthalpy) and decreases with increasing oxide thickness.

Building upon RIL 0401, revised empirically-based PCMI fuel failure criteria were developed separately for PWR and BWR fuel rod designs. Figure 3.1-3 provides the revised PWR PCMI fuel failure criteria in units of fuel enthalpy rise (Δcal/g) versus oxide-to-wall thickness. The supporting RIA empirical database, excluding the NSRR BWR Zircaloy-2 cladding specimens (FK-*n*, TS-*n*, and ATR-*n*), is included on Figure 3.1-3. The ratio of oxide thickness to cladding thickness was selected to capture the wide variations in fuel rod design within the empirical database (cladding thickness: 495 - 915 microns) because cladding stress is proportional to wall thickness.

Figure 3.1-4 depicts the proposed PCMI failure criteria against the empirical data - portions of which were scaled in accordance with RIL 0401. As mentioned above, PCMI failure will be less limiting at low corrosion levels than non-PCMI failure mechanisms. Examination of Figure 3.1-4 reveals that no PCMI fuel specimen failures were reported below an oxide/wall ratio of 0.04 (approximate 23 micron oxide layer on modern PWR 17x17 fuel designs). Above this amount of corrosion, PCMI becomes the dominant failure mechanism.

The proposed PWR PCMI cladding failure criteria, depicted in Figure 3.1-4, is initially anchored to the non-PCMI failure criteria (discussed above) and begins to decrease as PCMI becomes the dominant failure mechanism. Note that PCMI failure is related to change in fuel enthalpy (as opposed to total fuel enthalpy) and that the initial 150 Δcal/g corresponds to approximately 170 cal/g (non-PCMI criteria) for an event initiated at hot zero-power conditions. The non-PCMI failure criteria for rods with an internal pressure greater than system pressure, 150 cal/g, would be even more limiting than the criteria depicted in Figure 3.1-4.

As oxidation levels increase and absorbed hydrogen exceeds solubility and forms hydrides, PCMI becomes the dominant failure mechanism and the proposed failure criteria decreases. In determining the PWR PCMI failure criteria for normal operating conditions, it was recognized that the temperature effects of the cold NSRR test conditions may need to be further evaluated. Examination of Figure 3.1-4 reveals that the new failure criteria passes through or below a majority of the failed fuel specimens as well as several fuel specimens which did not fail. Several of the failed NSRR test results fall below the proposed criteria. At the cold NSRR test conditions (20 °C), even cladding with limited corrosion may exhibit hydrides which would normally be in solution at elevated, operating temperatures. Hence, these NSRR test specimens would exhibit lower ductility due to both hydrides (which would not be present at operating temperatures) and temperature effects.

Figure 3.1-5 illustrates the effect of temperature on measured elongation during burst test on irradiated Zr-4 tubing. This figure was provided by EPRI during a public workshop. The proposed PWR PCMI cladding failure criteria may not account for the full potential of temperature effects. Upon availability of results from scheduled RIA tests in NSRR's hot capsule program, the inclusion and scaling of the cold NSRR data points will be re-evaluated. It is anticipated that these tests will provide a benchmark to further scale the previous cold test results and allow a less restrictive (higher) failure criteria than currently proposed.

The inclusion of Cabri test results from MOX fuel specimens in the development of the PWR PCMI failure criteria was questioned by EPRI at a public workshop. Exclusion of REP-Na7, by itself, would not significantly effect the failure criteria. However, combined with a potential re-scaling of the NSRR results, the impact on PCMI failure thresholds at moderate corrosion levels may be significant. Potential MOX effects and the inclusion of these test results should be evaluated in the future.

Figure 3.1-6 provides a comparison of the proposed PWR PCMI failure criteria, RIL 0401 failure threshold, and a limit proposed by EPRI. Differences relative to RIL 0401 are due mostly to the exclusion of cold NSRR test results on BWR Zircaloy-2 fuel specimens. EPRI's proposed 95% statistical lower bound failure limit (based upon mechanistic fuel performance models and separate-effects mechanical properties) provides further assurance of the conservatism of the interim criteria. Note that the staff has not reviewed EPRI's lower bound failure limit to ensure

that the methods are conservative and that the statistics ensure a 95% lower bound. It is provided solely for comparison to the empirically-based criteria.

Core physics parameters are calculated as a function of cycle depletion. In order to convert an oxide-dependent criteria to a more useable burnup-dependent parameter, a good understanding of oxidation kinetics is required. Since cladding oxidation is dependent on both cladding alloy properties and plant-specific parameters such as operating temperature and coolant chemistry, each licensee will be required to submit an oxidation model similar to Figure 3.1-7. As part of this amendment request, the licensee will need to demonstrate that the hydrogen pickup fraction and hydride characteristics for their specific cladding alloy are similar to those exhibited by the alloys comprising the empirical database. A best-estimate nodal oxide thickness is judged sufficient to address the local cladding properties and convert the failure criteria to burnup. Nodal refers to a typical core neutronics model axial node (approximately 6 inches). Figure 3.1-8 illustrates the conversion of the revised failure criteria in Figure 3.1-4 to burnup for a modern PWR fuel rod design using two different cladding alloys (oxidation models in Figure 3.1-7).

BWR Fuel PCMI Failure:

As oxidation levels increase and absorbed hydrogen exceeds solubility and forms hydrides, PCMI becomes the dominant failure mechanism. Whereas hydrogen pickup in PWRs is well characterized, a correlation of measured oxide thickness to absorbed hydrogen concentration in BWR fuel is more elusive. Measurements on BWR Zr-2 fuel have shown a wide range in hydrogen concentration for similar burnup (and similar oxide thickness). Furthermore, improvements in manufacturing process have altered the corrosion properties of modern BWR Zr-2 cladding as compared to the Zr-2 cladding included in the NSRR RIA test program. As a result, the BWR PCMI failure criteria will be correlated to hydrogen concentration as opposed to the oxide/wall ratio employed for the PWR criteria. Each licensee will be required to submit a corrosion model which correlates hydrogen concentration to burnup for their specific cladding alloy. The effects of plant specific operating conditions and chemistry will need to be addressed as part of this license amendment. Similar to PWR oxidation, a best-estimate nodal hydrogen concentration is judged sufficient to address the local cladding properties.

The proposed empirically-based BWR PCMI fuel failure criteria is depicted in Figure 3.1-9 along with the supporting NSRR BWR Zr-2 RIA database. Where hydrogen content on the NSRR specimens was reported as a range (e.g. FK-10 reported 141-220 ppm), this range is depicted by a line in Figure 3.1-9. The proposed failure criteria conservatively bounds the failure data at the lowest reported hydrogen content. Hydrogen data reported in References 6, 7, and 8.

Figure 3.1-10 compared the proposed failure criteria against an expanded database including BIGR and IGR test results. In combination with the NSRR data, the IGR and BIGR empirical data provides a basis for determining the point at which PCMI becomes the dominant failure mechanism (relative to hydrogen concentration). Note that the hydrogen concentration for the IGR specimens is unknown; however expected to be similar to the BIGR (both of which had minimal oxide layers). Examination of Figure 3.1-10 reveals that no PCMI fuel specimen failures were reported below a minimum hydrogen content of 141 ppm (range of 141-220 ppm). However, based on the limited database, the point at which PCMI becomes the dominant failure

mechanism was set at 75 ppm. Above 75 ppm, the failure criteria decreases significantly in order to bound the reported failure data. At hydrogen levels beyond the NSRR database, the PCMI failure criteria continues to decrease in order to account for the continuing hydride embrittlement of the cladding.

With the exception of FK-10 (80 °C) and FK-12 (85 °C), the database supporting the BWR cladding failure criteria were all conducted from an initial temperature of 20 °C - consistent with cold startup BWR conditions. Due to temperature and hydrogen solubility effects, application of the BWR cladding failure criteria to higher operating temperatures is conservative. Future evaluation of hydrogen solubility and temperature effects may be pursued in order to refine the BWR PCMI failure criteria for application to higher operating temperatures. Another potential conservatism in the proposed criteria is the short NSRR pulse width relative to the broader pulse width of operating BWRs.

Figure 3.1-1: Non-PCMI Fuel Cladding Failure Criteria - Empirical Database

(PCMI Failures Removed)

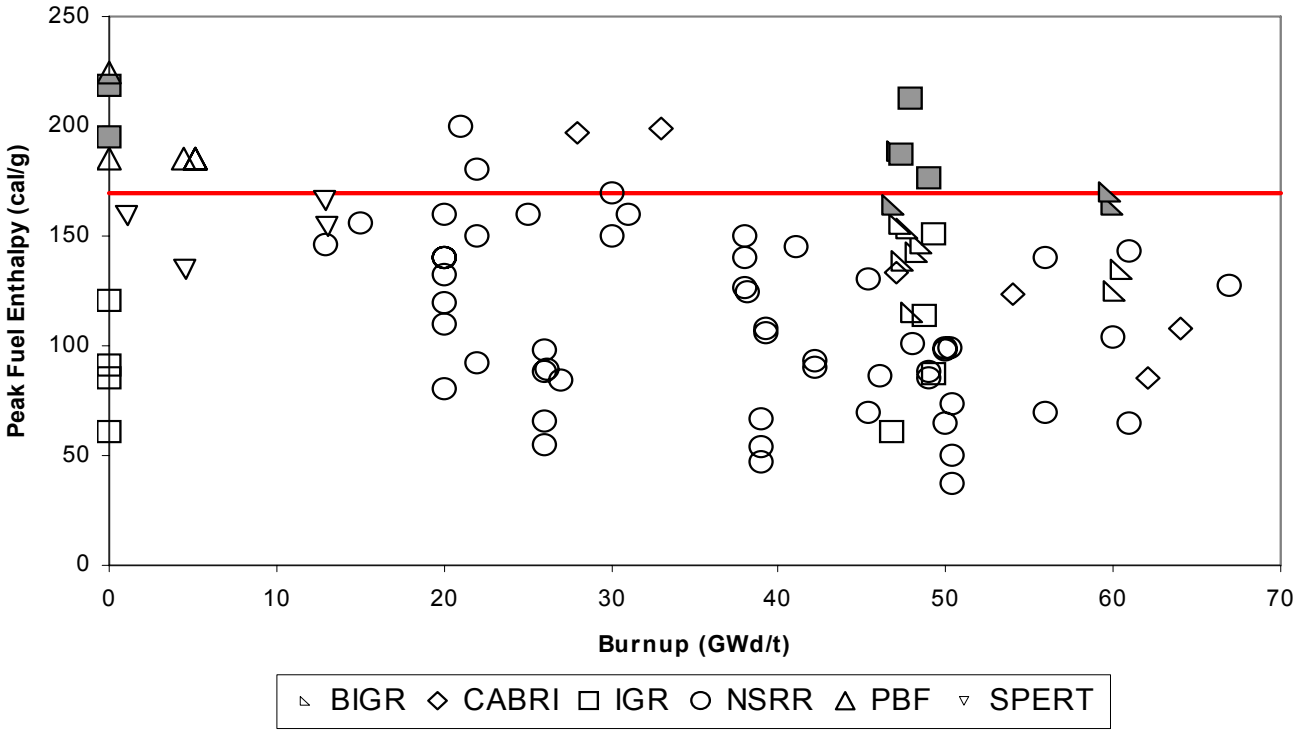

Figure 3.1-2: High Cladding Temperature Failure Versus Differential Pressure

(Slide from EPRI presentation at RIA Workshop #2, December 19, 2006)

EPRI

High Temperature Ballooning Failures

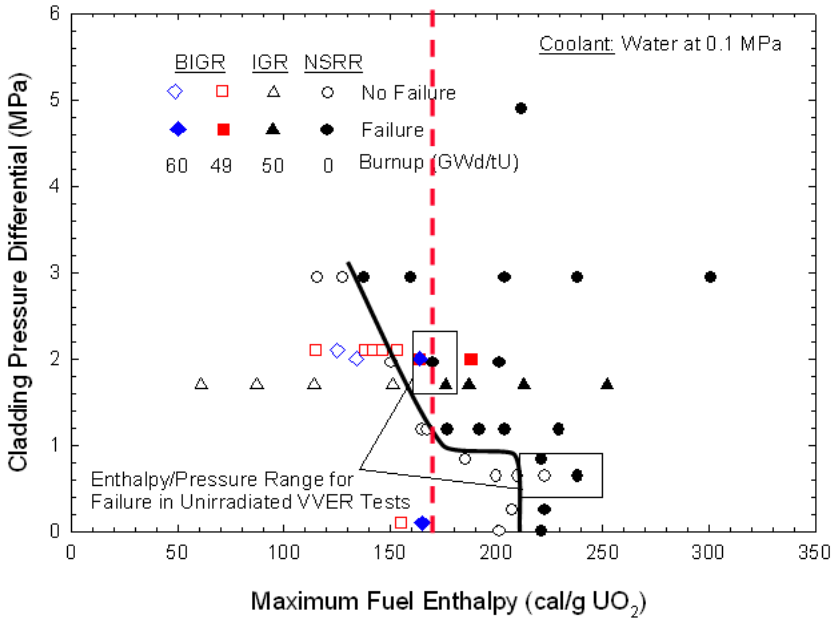

Figure 3.1-3: PCMI Fuel Cladding Failure Criteria - PWR

(raw empirical data, BWR Zr-2 tests not included)

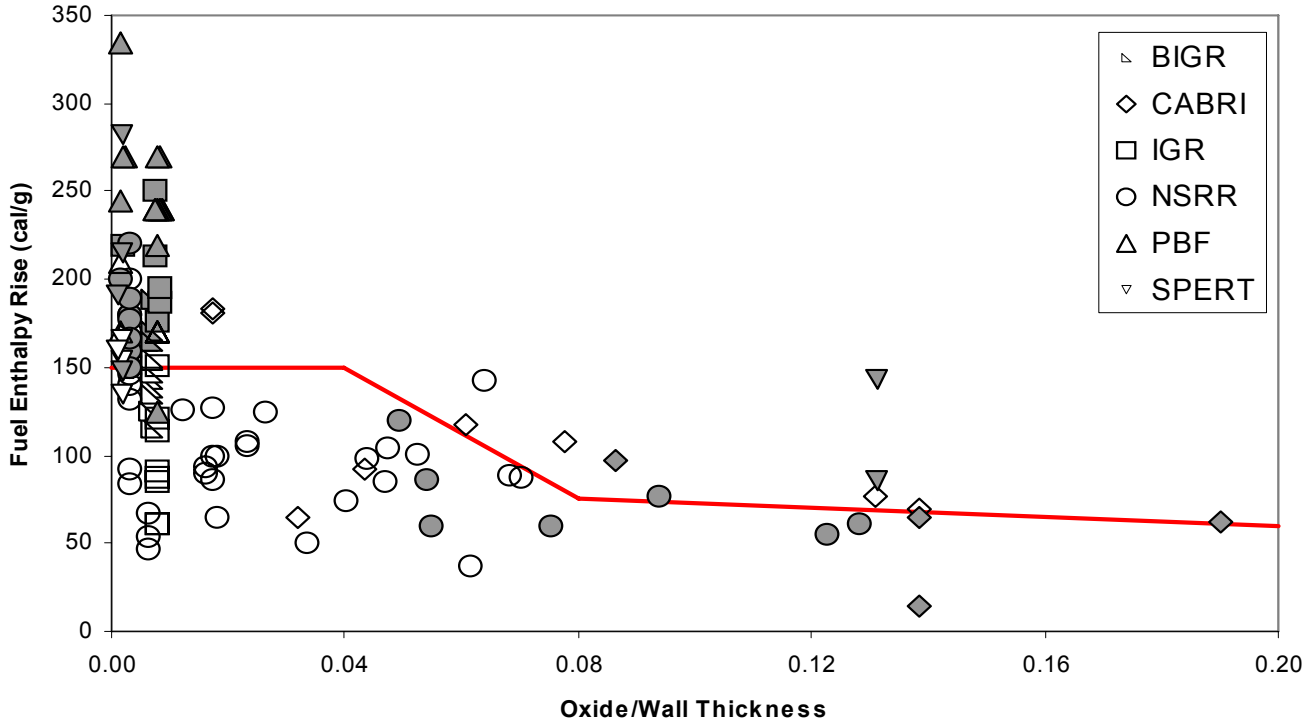

Figure 3.1-4: PCMI Fuel Cladding Failure Criteria - PWR

(scaled empirical data based on RIL0401, BWR Zr-2 tests not included)

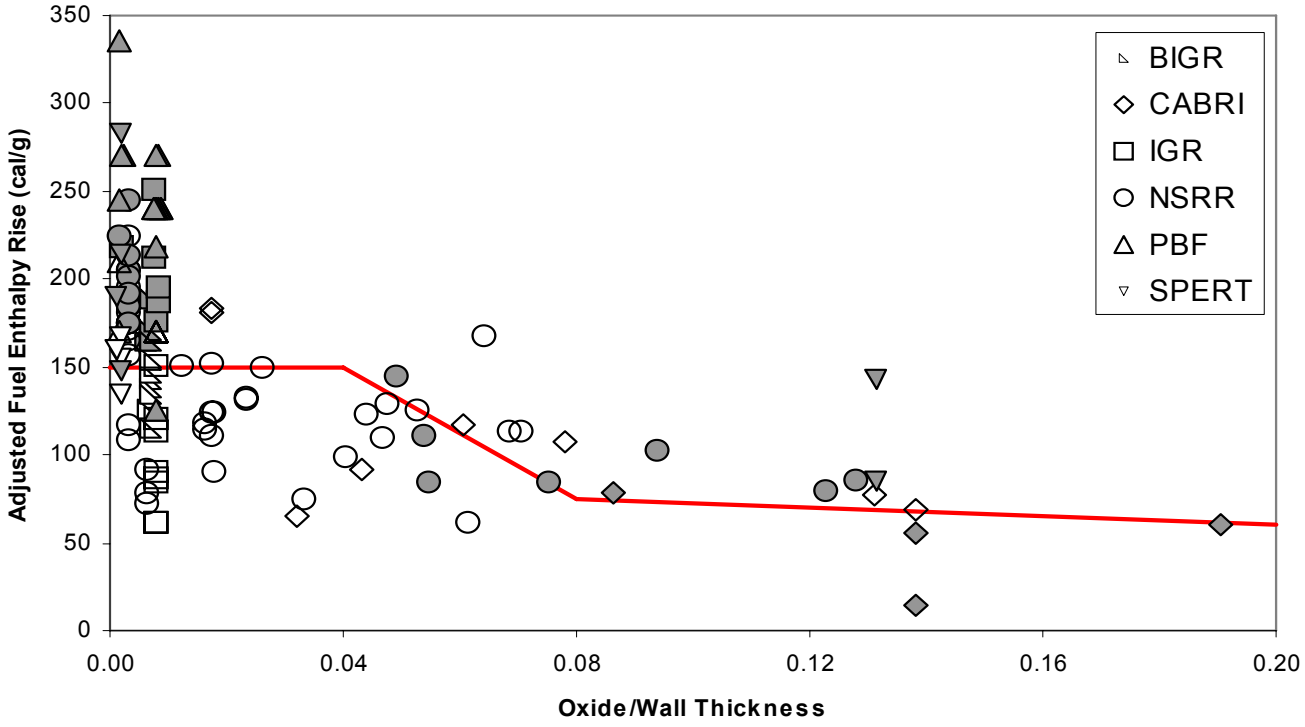

O/W Ratio	Failure Criteria Breakpoints
0.00	150
0.04	150
0.08	75
0.20	60

Figure 3.1-5: Temperature Effects on Burst Test Results

(Slide from EPRI presentation at RIA Workshop #2, December 19, 2006)

EPRI

Impact of Temperature on Total Elongation

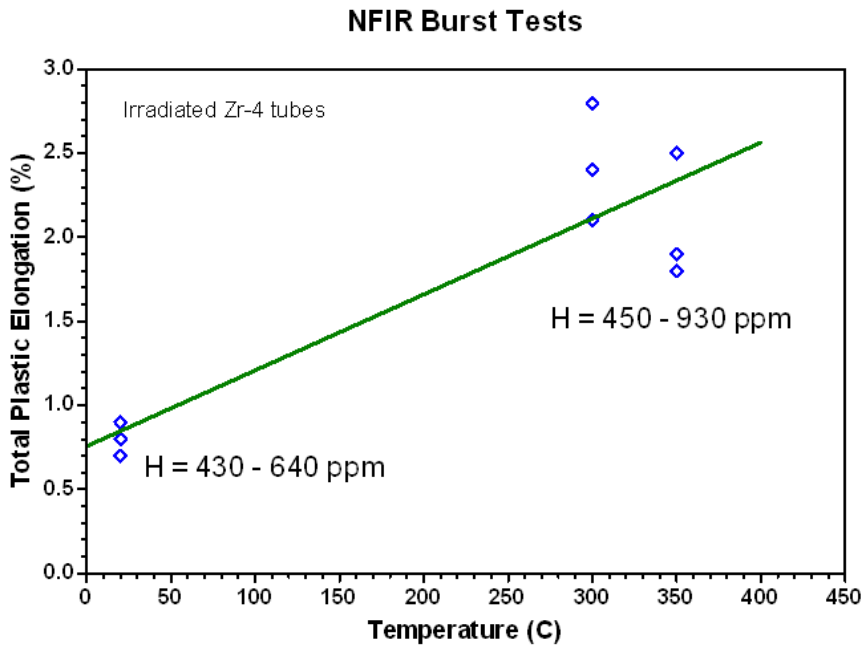

Figure 3.1-6: Comparison of Fuel Cladding Failure Criteria - PWR

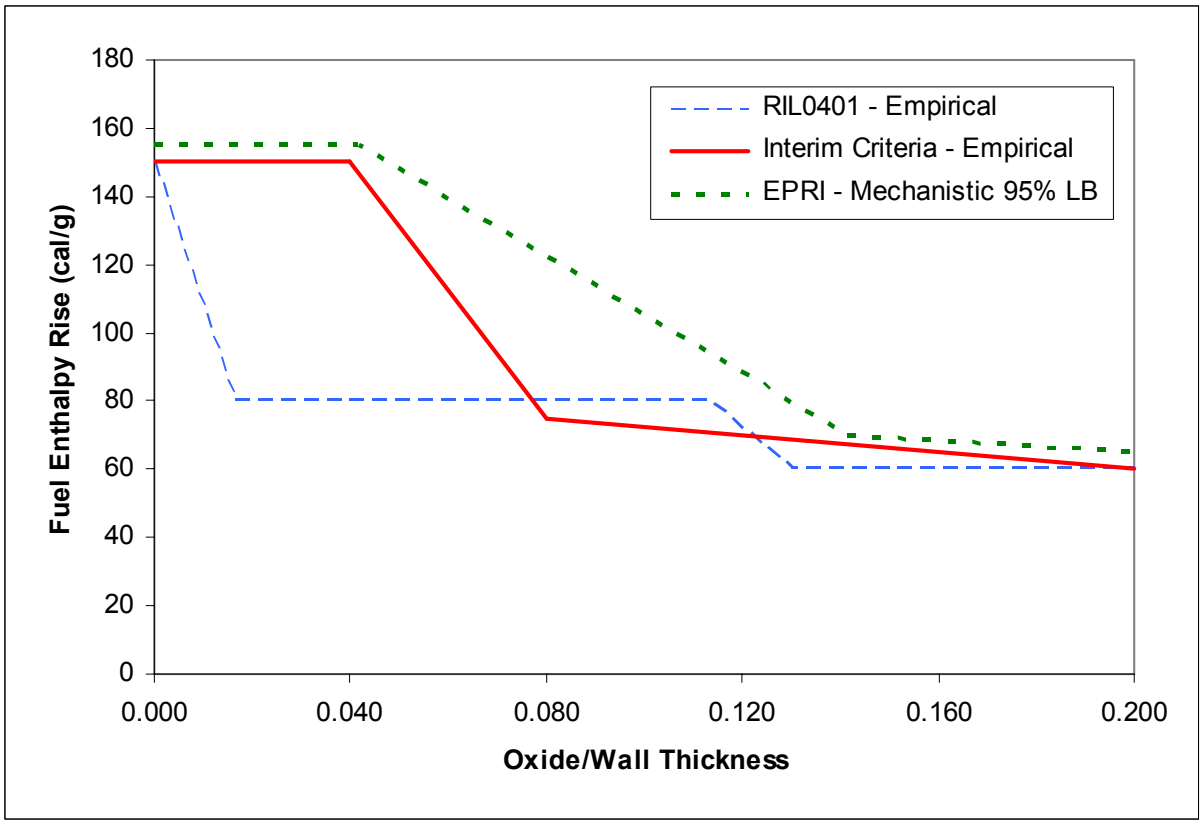

Note: EPRI proposed lower bound PWR cladding failure limit based on presentation at RIA Public Workshop (November 9, 2006).

Figure 3.1-7: Typical PWR In-Service Corrosion

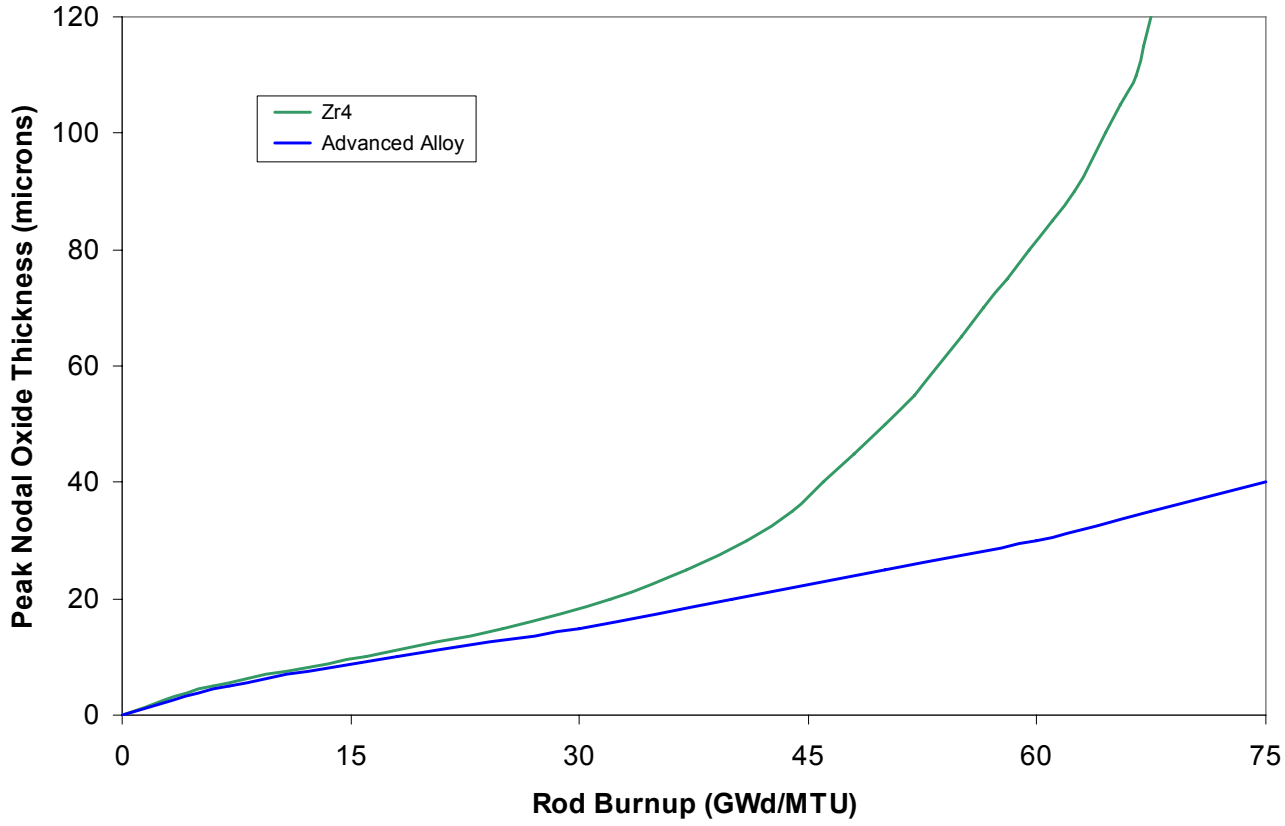

Figure 3.1-8: Fuel Failure Criteria - Converted to Rod Average Burnup

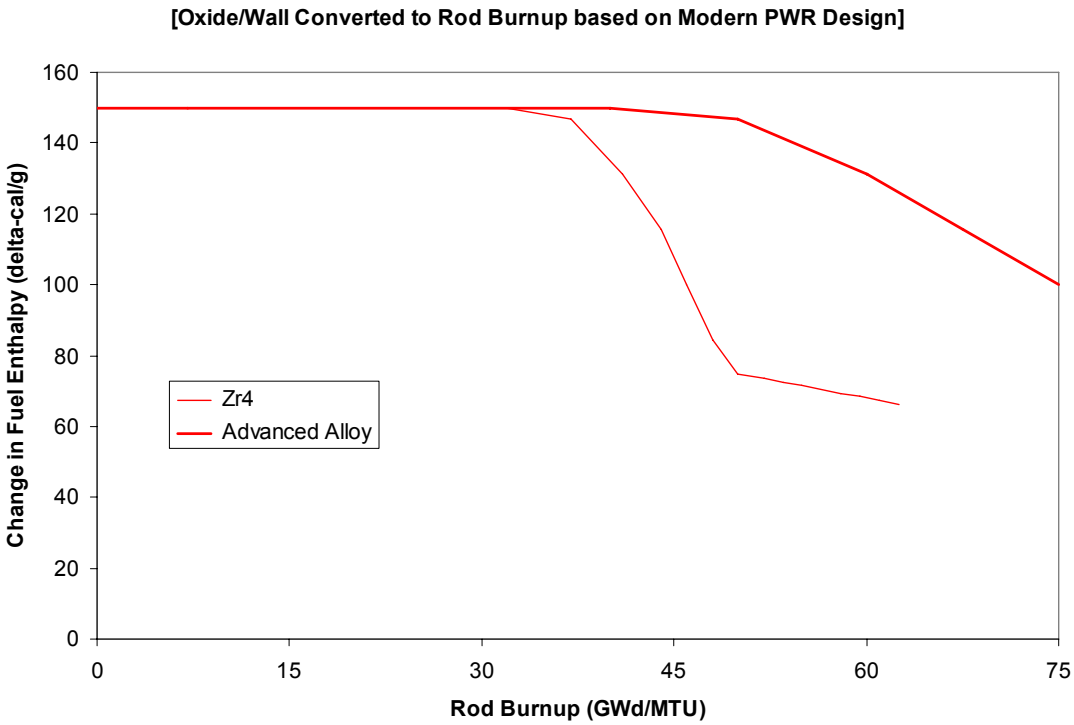

Figure 3.1-9: PCMI Fuel Cladding Failure Criteria - BWR

(raw empirical data, NSRR BWR Zr-2 specimens)

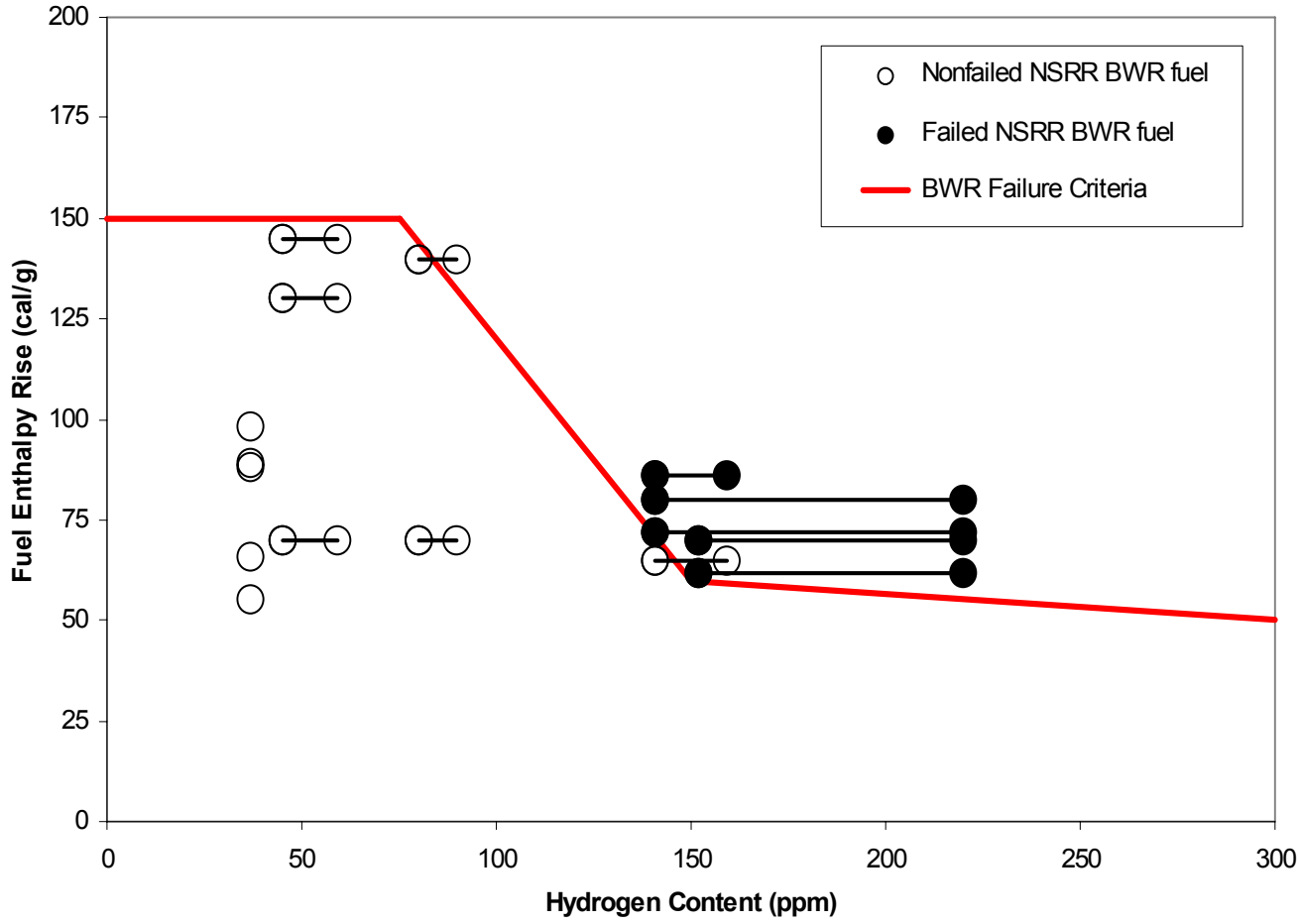

Hydrogen Content (ppm)	Failure Criteria Breakpoints
0	150
75	150
150	60
300	50

Figure 3.1-10: PCMI Fuel Cladding Failure Criteria - BWR

(raw empirical data, U.S. PWR tests not included)

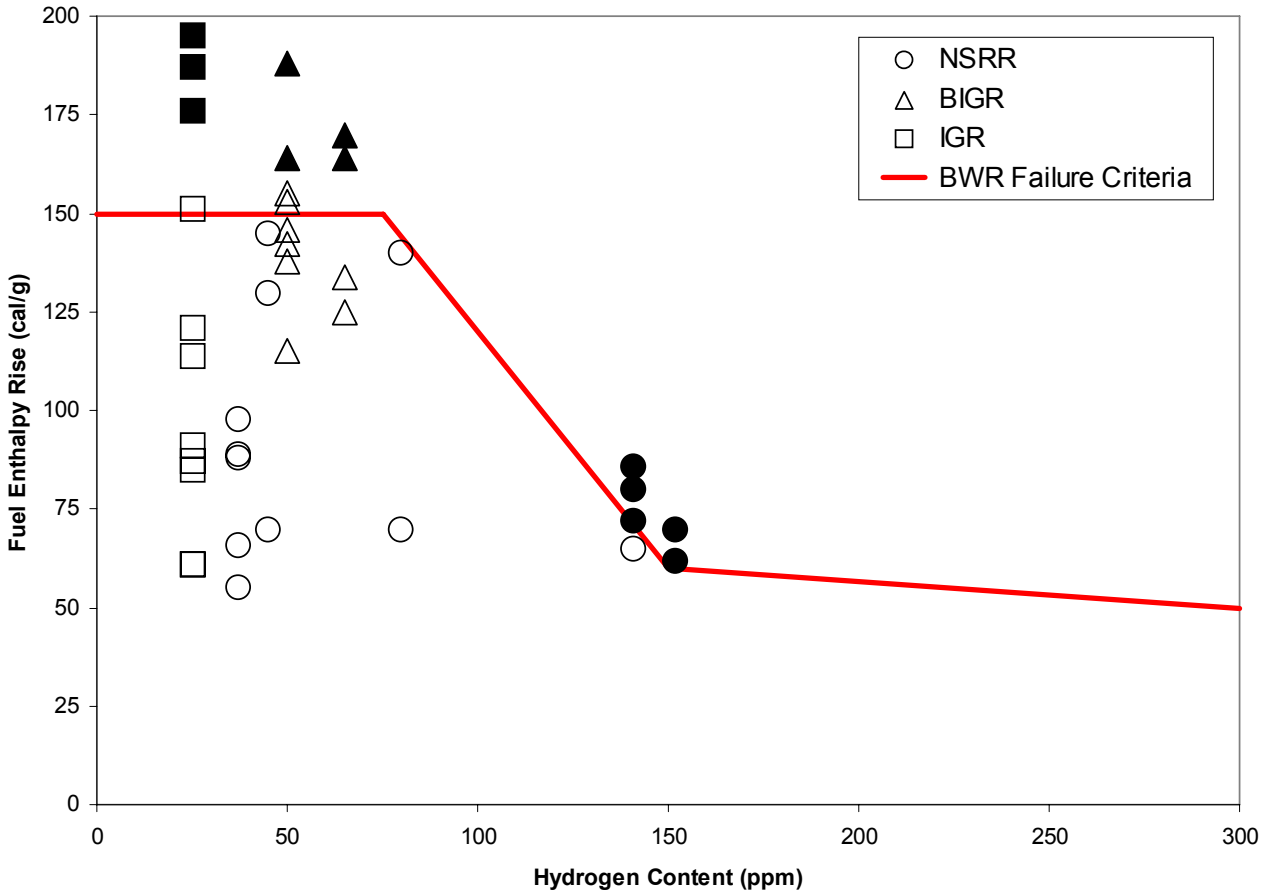

3.2 Coolable Core Geometry

During a prompt critical power excursion, the following phenomena may challenge the structural integrity of the reactor pressure boundary and ability to maintain a coolable core geometry:

1. Pressure pulse generated by the violent expulsion of molten or near molten fuel fragments and ensuing interaction with reactor coolant.
2. Flow blockage due to fission product-induced swelling of molten fuel coupled with cladding plastic deformation.
3. Fuel powdering and dispersal within the reactor coolant system.

Figure 3.0-1 illustrates the extent of the RIA empirical database. While many international research programs have generated RIA test results, no facility since PBF (1978 - 1980) has targeted nor achieved fully molten fuel and loss of fuel rod geometry. As a result, the empirical database supporting the development of a coolability criteria is limited to earlier, domestic, low burnup test results. Based upon MacDonald's evaluation of SPERT, TREAT, and PBF test results (See Section 3.0), an upper limit on peak radial average fuel enthalpy of 230 cal/g is required to ensure a coolable core geometry.

3.2.1 Interim Criteria

Based upon an assessment of the RIA empirical database and building upon RIL 0401, the following core coolability criteria are proposed.

1. **Peak radial average fuel enthalpy must remain below 230 cal/g.**
2. **Peak fuel temperature must remain below incipient fuel melting conditions.**
3. **Mechanical energy generated as a result of (1) non-molten fuel-to-coolant interaction and (2) fuel rod burst must be addressed with respect to reactor pressure boundary, reactor internals, and fuel assembly structural integrity.**
4. **No loss of coolable geometry due to (1) fuel pellet and cladding fragmentation and dispersal and (2) fuel rod ballooning.**

Fuel rod thermal-mechanical calculations must be based upon design-specific information accounting for manufacturing tolerances and modeling uncertainties using NRC approved methods including burnup-enhanced effects on pellet power distribution, fuel thermal conductivity, and fuel melting temperature.

3.2.2 Technical Basis

RIL 0401 noted that "expanding fission gas bubbles can disperse fuel particles from high-burnup fuel during an RIA pulse, whereas molten fuel expansion was required to disperse fuel particles from low-burnup fuel." MacDonald concluded that loss of rod geometry and flow blockage could occur below fuel melting conditions. Building upon both of these assessments, the interim coolability criteria will need to capture both low-burnup phenomena (e.g. loss of rod geometry and molten fuel-to-coolant interaction) and high-burnup phenomena (e.g. fuel powdering and dispersal, and high rod internal pressure).

The Electric Power Research Institute (EPRI) proposed revised RIA fuel failure and core coolability criteria (Reference 3). In Section 4 of this topical report, EPRI describes the technical bases for a revised core coolability limit including the empirical database supporting the FCI mechanical conversion (consisting of both out-of-pile and in-pile experiments). EPRI notes that these experiments have shown that the rapid generation of vapor leading to large coolant pressure pulses depends on the particle size of the dispersed material, the energy of the dispersed material, and the coolant conditions, primarily, the amount of water to fuel ratio and the coolant subcooling. EPRI concludes that although it is possible to disperse into the coolant a small fraction of the fuel pellet as finely fragmented particles, the empirical database demonstrates that dispersal of non-molten material is less efficient in converting the thermal energy in the fuel particles to mechanical energy in the coolant. As a result, EPRI proposed a coolability criteria which would preclude incipient fuel melting.

Incipient Fuel Melting:

In Section 4.2.2 of the EPRI topical report, the FALCON code is used to calculate the radial average fuel enthalpy at incipient melting conditions. The influence of fuel burnup on pellet thermal conductivity, pellet power distribution, and fuel melting temperature were explicitly addressed. Sensitivity studies to evaluate the effects of outer surface oxide thickness or DNB heat transfer demonstrated that the variations in cladding-to-coolant heat transfer conditions had no impact on the radial average peak fuel enthalpy necessary to cause local incipient melting. Figure 3.2-1 depicts the EPRI calculated fuel enthalpy necessary to induce incipient melting for a 20 ms pulse width and 10 ms pulse width (based on pulse width sensitivity cases, Section 4.3.1.4 of Reference 3). Figure 3.2-1 also depicts the current RG 1.77 criteria and the coolability limit proposed by MacDonald.

By precluding incipient fuel melting, phenomena challenging long-term core coolability and integrity of the reactor pressure boundary are reduced (but not eliminated). Since fuel temperature calculations are dependent on fuel rod design, power history, burnup, initial rod conditions, and the amount and rate of reactivity insertion, design specific calculations need to be prepared in order to ensure that local fuel temperatures remain below incipient melting conditions. These fuel rod thermal-mechanical calculations must be based upon design-specific information accounting for manufacturing tolerances and modeling uncertainties using NRC approved methods including burnup-enhanced effects on pellet power distribution, fuel thermal conductivity, and fuel melting temperature. While performing these calculations, it is important to consider that, due to a burnup-dependent, non-uniform pellet radial power profiles, the peak fuel temperature may not occur at the centerline under transient conditions.

The EPRI topical report, which has not been formally reviewed and approved by the NRC staff, concludes that the dispersal of non-molten fuel fragments is of less significance than molten FCI. Nonetheless, the mechanical energy associated with non-molten fuel dispersal must be quantified. In addition to a coolability criterion on peak fuel enthalpy (MacDonald's 230 cal/g to preserve fuel bundle geometry) and a coolability criterion of no fuel melting (to prevent molten FCI), criteria must be developed to address the dispersal of finely fragmented non-molten fuel particles and fuel rod ballooning and rupture. The following criteria are proposed:

- Mechanical energy generated as a result of (1) non-molten fuel-to-coolant interaction and (2) fuel rod burst must be addressed with respect to reactor pressure boundary, reactor internals, and fuel assembly structural integrity.
- No loss of coolable geometry due to (1) fuel pellet and cladding fragmentation and dispersal and (2) fuel rod ballooning.

Since disposition of these two coolability criteria would require fuel design specific and plant design specific evaluations, each licensee would be required to demonstrate compliance with these two coolability criteria as well as the previous two criteria. Alternatively, bounding evaluations encompassing many plant and fuel designs may be submitted for NRC review. It is important to recognize that the empirical database related to FCI is limited such that an accurate prediction of mechanical energy will be difficult to justify without further experimental data.

The following section briefly describes the RIA empirical database with respect to fuel fragmentation and dispersal.

Fuel Dispersal:

Examination of the RIA empirical database (See Section 3.0) reveals a significant number of failed fuel specimens. Twelve of the specimens tested at NSRR, CABRI, IGR, and BIGR experienced fuel dispersion (not including SPERT and PBF tests beyond 230 cal/g). Figure 3.2-2 and 3.2-3 illustrate the fuel dispersal database as a function of peak fuel enthalpy versus burnup and pulse width respectively. RIL 0401 investigated fuel dispersal and concluded that "prompt heating of fission gas bubbles that accumulate at high burnup on grain boundaries can explode the grain structure, driving fuel particles into the coolant under certain conditions." Examination of Figure 3.2-2 reveals that no fuel specimens below a burnup of 30 GWd/MTU experienced fuel dispersal. Examination of Figure 3.2-3 reveals that no UO_2 fuel specimens experienced fuel dispersal when exposed to a pulse width greater than 10ms. REP-Na-7, a MOX fuel specimen, experienced fuel loss at a pulse width of 40 ms.

The fuel pellet peripheral rim undergoes a restructuring at elevated burnup. The resulting "rim region" consists of a high density of grain boundaries and fission gas filled pores which is more susceptible to grain boundary separation and fuel powdering during an RIA. Coupled with an edge-peaked radial power peaking, higher burnup fuel pellets may experience dispersion of finely fragmented fuel particles at a fuel radial average enthalpy below melting conditions.

Figure 3.2-4 provides measurements of the high burnup rim structure as a function of burnup. As shown in figures (a) and (b), the rim width is minimal below 40 Gwd/MTU. Hence, the amount of fuel material within each fuel pellet susceptible to fine fragmentation is minimal below 40 GWd/MTU.

The extent of the RIA empirical database with respect to fuel dispersal, 12 high-burnup fuel specimens for which a degree of fuel pellet loss had been reported, is illustrated in Figures 3.2-2 and 3.2-3. Several of these test specimens experienced large axial cracks in the cladding with a significant loss of fuel. The amount and size of dispersed fuel fragments is influenced by fuel enthalpy, fuel burnup (rim structure), and the extent of cladding failure. Precluding incipient fuel melting eliminates concerns associated with molten FCI. However, the effects of dispersing non-molten fuel fragments, whether finite rim structure or coarse pellet particles, must be considered with respect to GDC28 requirements on core coolability and reactor pressure integrity.

The scope of a technical evaluation demonstrating compliance to the coolability criteria may be reduced by demon strating fuel cladding integrity either in all cases or beyond a certain burnup. Alternatively, applicants may want to investigate the inherent characteristics of their power pulse and its effects on fuel dispersal. The applicant may also attempt to demonstrate that long-term cooling criteria: (1) fuel fragmentation with respect to flow blockage, (2) transport of dispersed fuel fragments within the primary coolant system, and (3) rod ballooning are bounded by another event of equal or higher probability. For this case, short-term coolability phenomena related to non-molten FCI and pressure pulse need to be addressed. In any RIA licensing strategy, applicants will need to address radiological consequences.

Figure 3.2-1: Coolable Core Geometry Fuel Enthalpy Limits

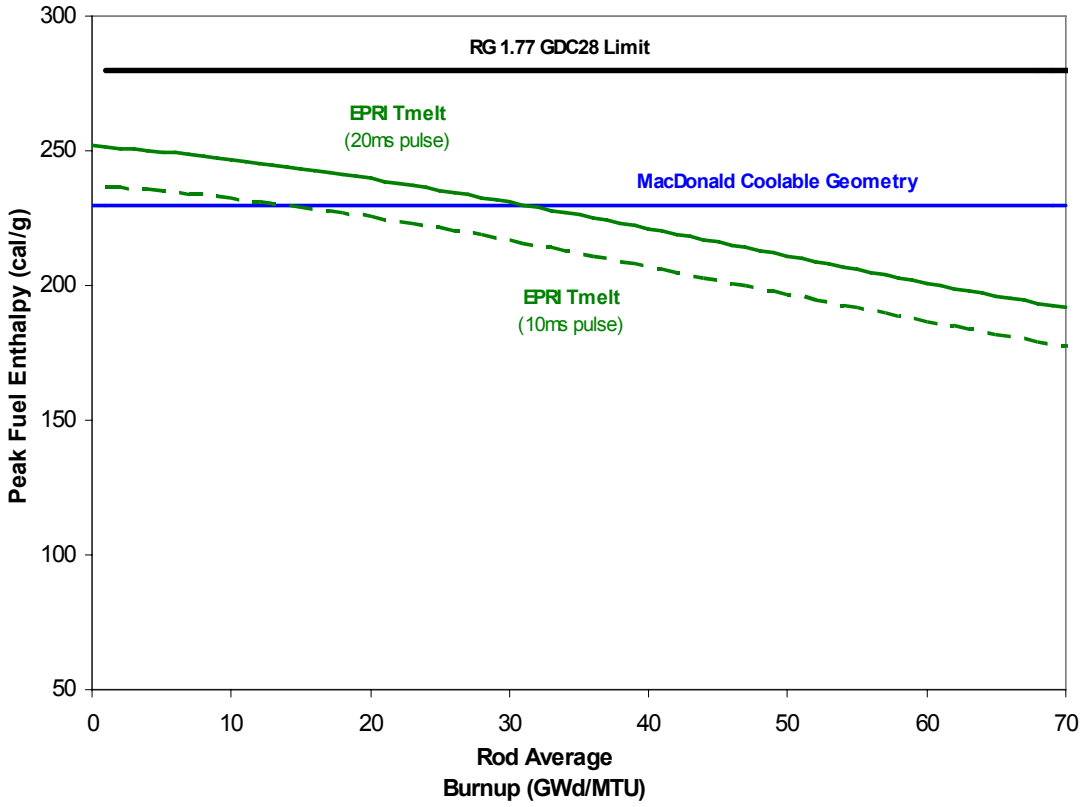

Figure 3.2-2: Fuel Dispersal: Fuel Enthalpy versus Burnup

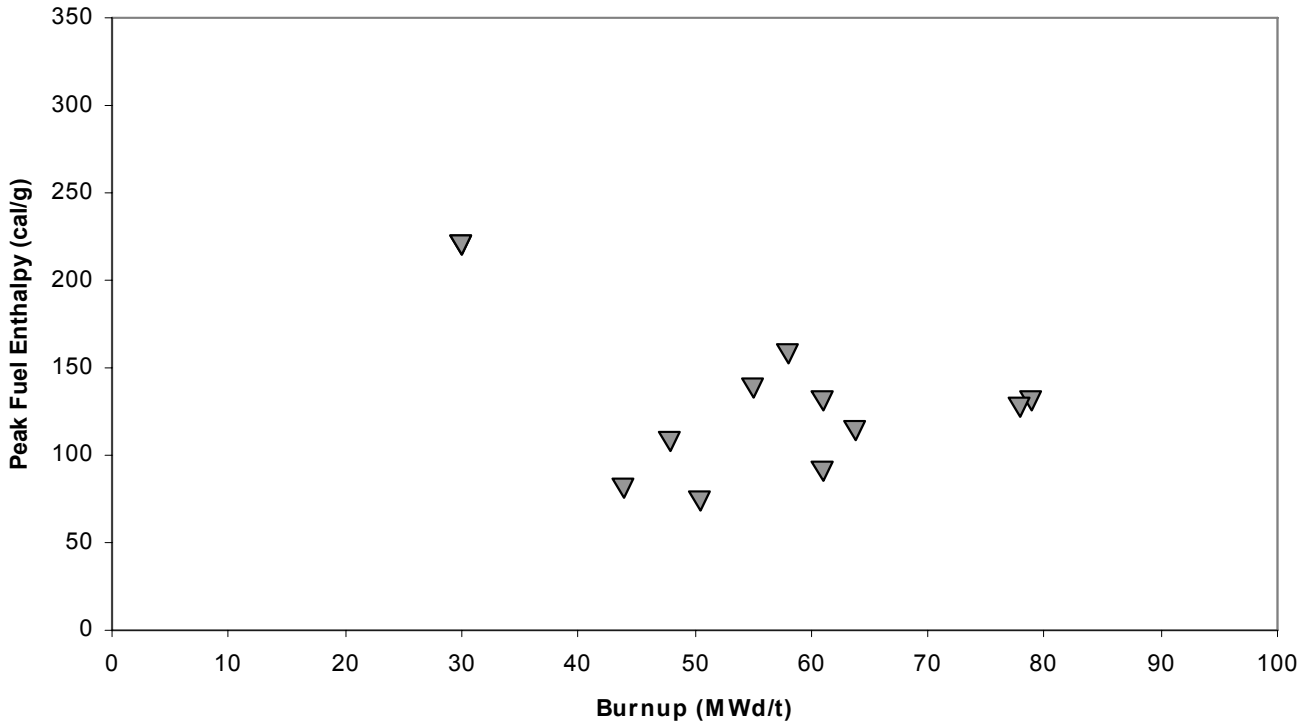

Figure 3.2-3: Fuel Dispersal: Fuel Enthalpy versus Pulse Width

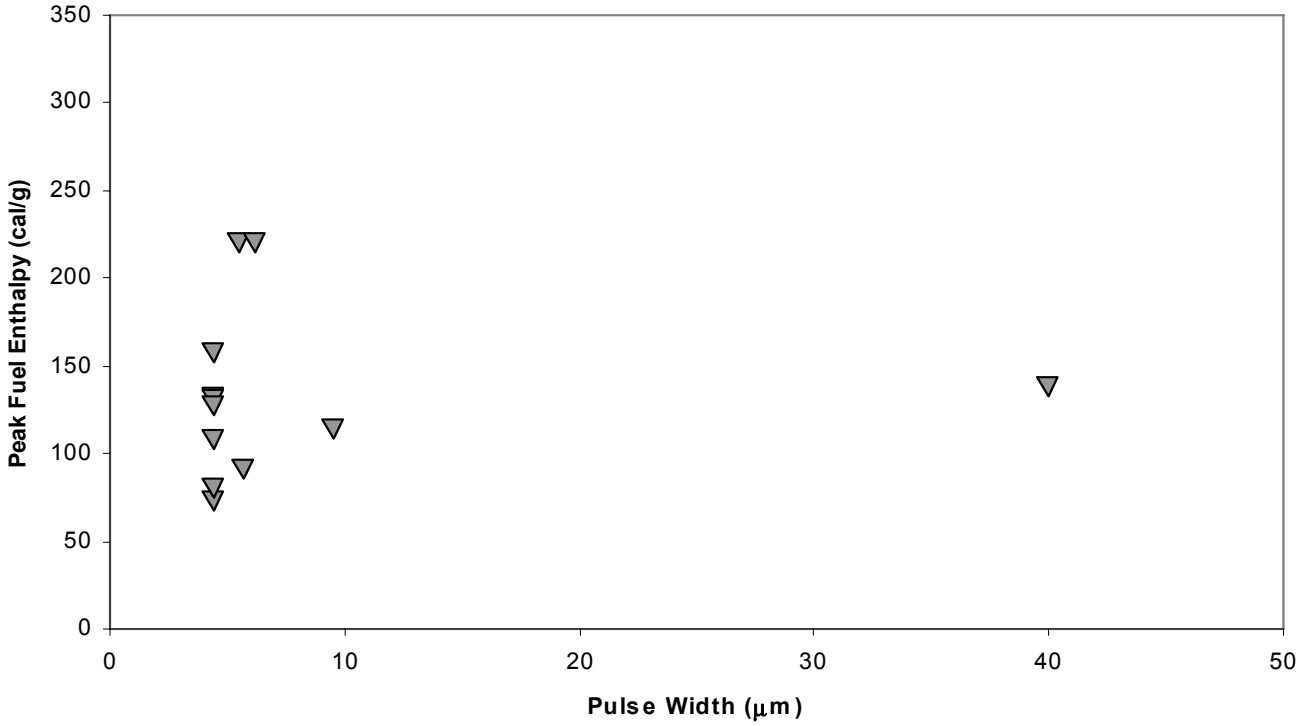

Figure 3.2-4: High Burnup Rim Structure

Figure (a) Optical microscopy on PWR fuel (Reference 4)

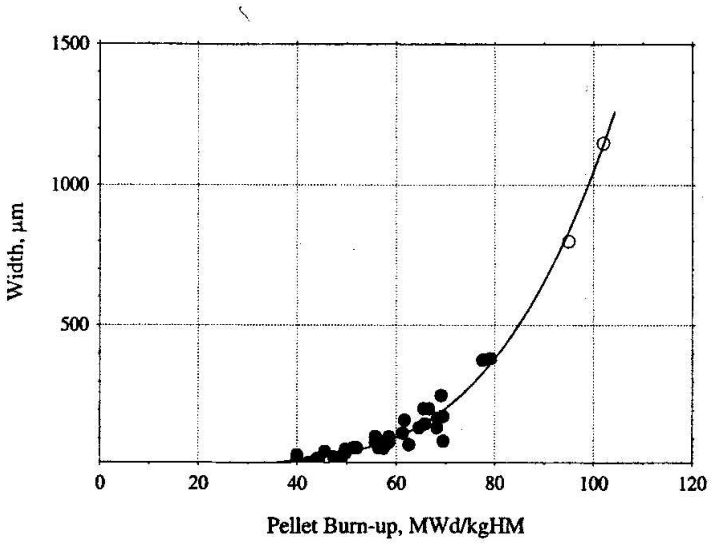

Figure (b) Burnup dependence of rim width (Reference 5)

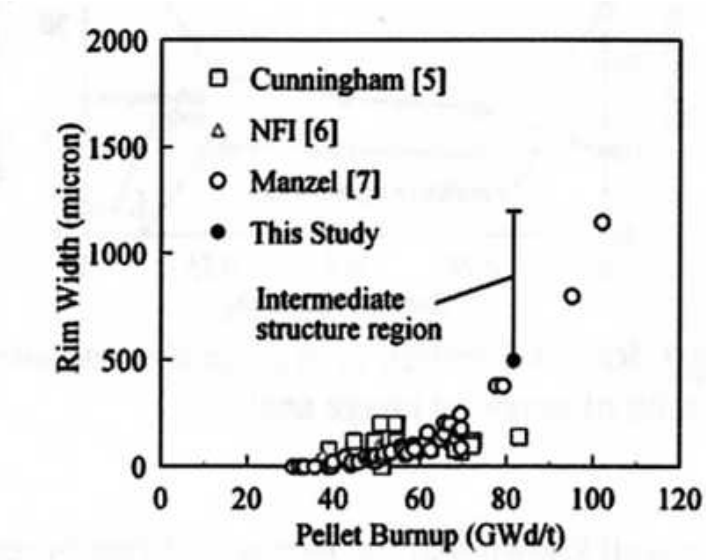

3.3 Radiological Fission Product Inventory

Appendix B to RG 1.77 (1974) provides guidance and assumptions for evaluating the radiological consequences of a control rod ejection accident. These assumptions are supplemented by guidance given in RG 1.183 (2000) and RG 1.195 (2003). Regulatory guidance related to fission-product gap inventory within these documents is listed below:

RG 1.77 Appendix B, Assumption 1.c:

> "*The amount of activity accumulated in the fuel-clad gap should be assumed to be 10% of the iodines and 10% of the noble gases accumulated at the end of core life, assuming continuous maximum full power operation.*"

RG 1.183 Table 3:

> "*The release fractions listed here have been determined to be acceptable for use with currently approved LWR fuel with a peak burnup up to 62,000 MWD/MT U provided that the maximum linear heat generation rate does not exceed 6.3 kw/ft peak rod average power for burnups exceeding 54 GWD/MTU. As an alternative, fission gas release calculations performed using NRC approved methodologies may be considered on a case-by-case basis. To be acceptable, these calculations must use a projected power history that will bound the limiting projected plant-specific power history for the specific fuel load. For the BWR rod drop accident and the PWR rod ejection accident, the gap fractions are assumed to be 10% for iodines and noble gases*."

Note similar statements concerning gap fraction contained in RG 1.183 Appendix C and H. This information is also stated within RG 1.195 (Table 2, Appendix C and H) for non-alternate source term applications.

The total fission-product gap fraction available for release following any RIA would include the steady-state gap inventory (present prior to the event) plus any fission gas released during the event. The steady-state gap inventory would be consistent with the Non-LOCA gap fractions cited in RG 1.183 (Table 3) and RG 1.195 (Table 2) and would be dependent on operating power history.

Whereas fission gas release (into the rod plenum) during normal operation is governed by diffusion, pellet fracturing and grain boundary separation are the primary mechanisms for fission gas release during an RIA. Hence, the amount of release is dependent on local burnup (fission gas accumulation along grain boundaries and within the porous rim region) and local power increase.

Measurements of fission gas release were conducted on several of the CABRI, BIGR, and NSRR fuel specimens (non-failed specimens) following the RIA tests (References 6 through12). This empirical data is presented in Figures 3.3-1 through 3.3-3. Examination of these figures reveals a large spread in the measured data. Note that in most instances the fuel specimens were manufactured from commercial reactor fuel. While preparing the test specimens, prior operation fission product gap inventory was evacuated. Hence, the initial gap inventory is almost zero (some pre-conditioning of the fuel specimens) and the measured fission gas equals transient released fission gas.

Based upon the measured fission gas release, the staff developed the following correlation

between gas release and maximum fuel enthalpy increase:

Transient FGR = [(0.2286*ΔH) – 7.1419]

Where:

FGR = Fission gas release, % (must be $\geq$ 0)

ΔH = Increase in fuel enthalpy, Δcal/g

Figure 3.3-3 depicts this correlation against measured data.

Total fission-product inventory available for release upon cladding failure equals the steady-state gap inventory (from the applicable RG) plus the transient release (calculated with the above correlation). The transient release from each axial node which experiences the power pulse may be calculated separately and combined to yield the total transient FGR for a particular fuel rod. The combined steady-state gap inventory and transient FGR from every fuel rod predicted to experience cladding failure (all failure mechanisms) should be used in the dose assessment. Additional guidance is available within RG 1.183 and 1.195.

Figure 3.3-1: RIA Fission Gas Release Database - Rod Burnup

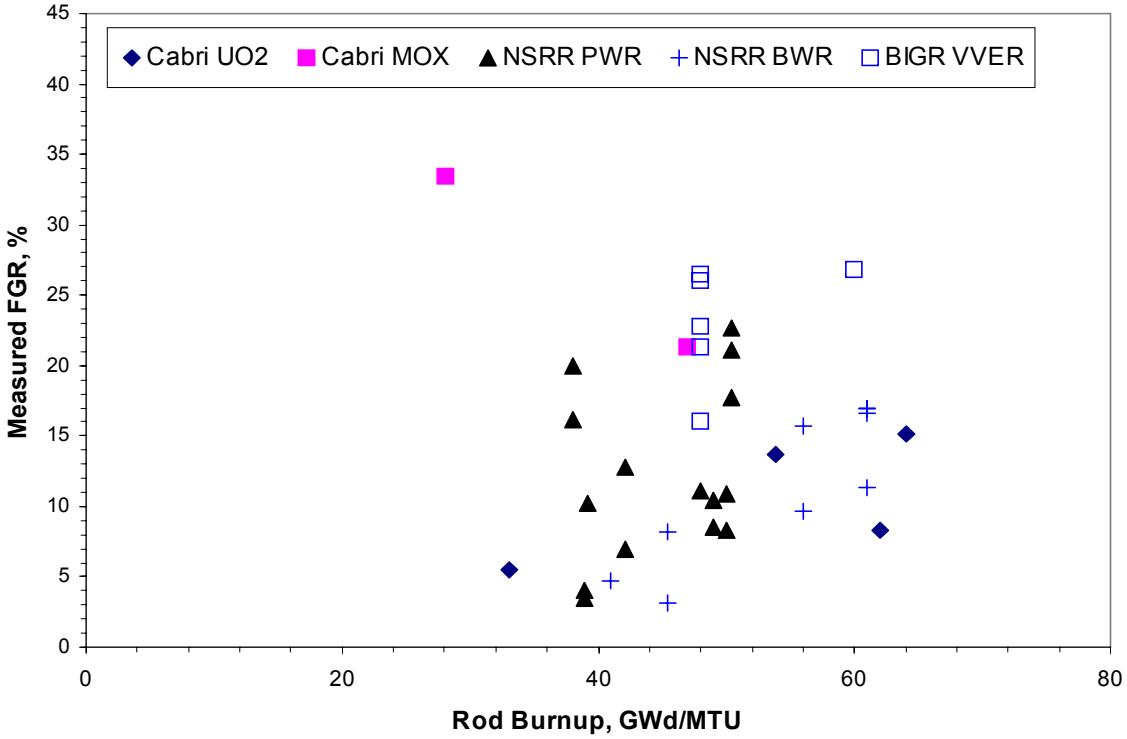

Figure 3.3-2: RIA Fission Gas Release Database - Pulse Width

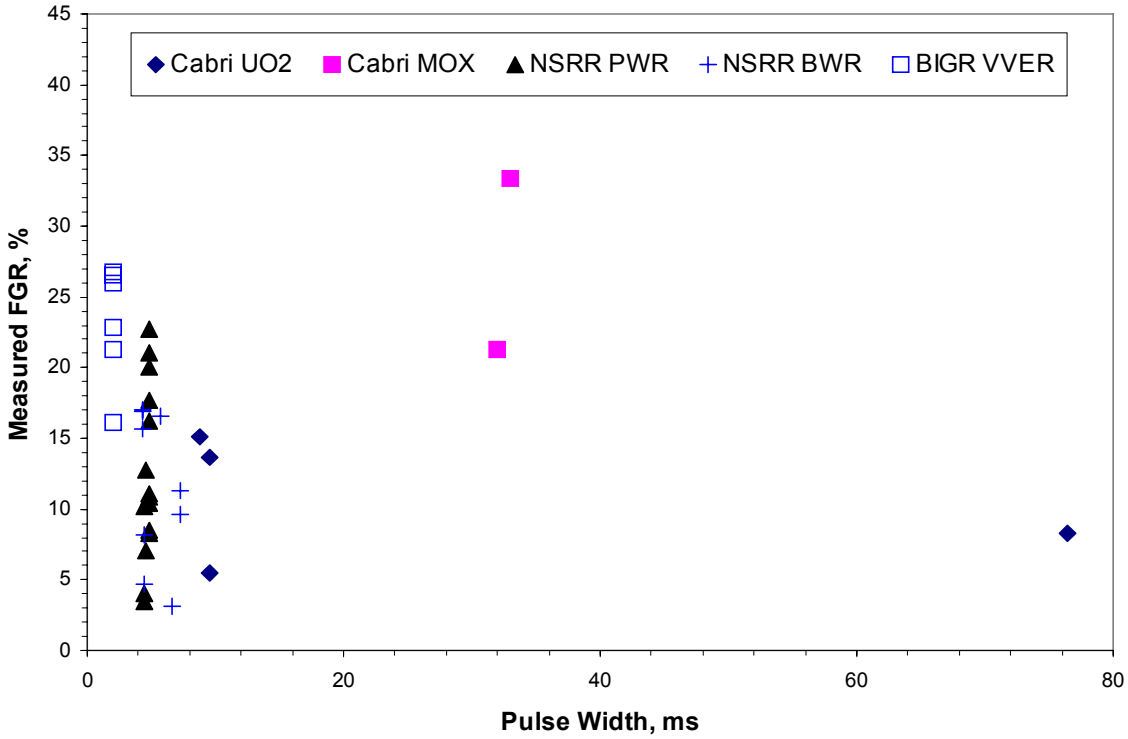

Figure 3.3-3: RIA Fission Gas Release Database - Increase in Fuel Enthalpy

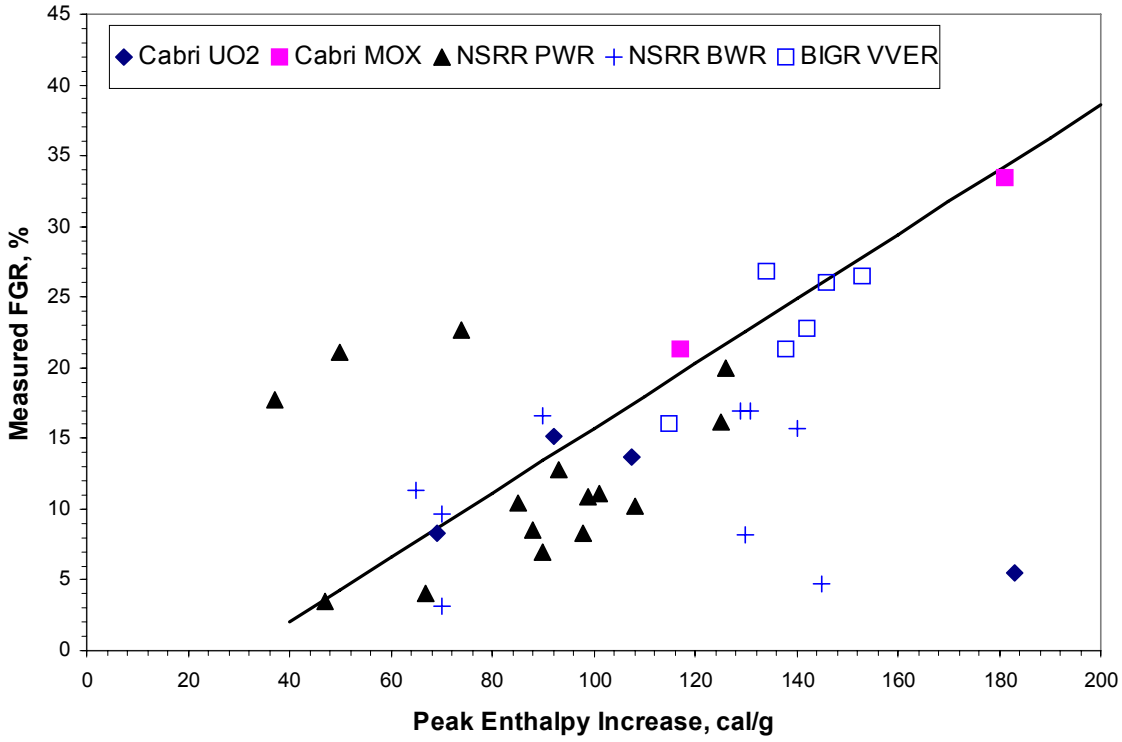

4.0 INTERIM ACCEPTANCE CRITERIA AND GUIDANCE

Based upon an assessment of the RIA empirical database and building upon RIL 0401, the following fuel cladding failure criteria and core coolability criteria were developed

Fuel Cladding Failure:

1. The high cladding temperature failure criteria for zero power conditions is a peak radial average fuel enthalpy greater than 170 cal/g for fuel rods with an internal rod pressure at or below system pressure and 150 cal/g for fuel rods with an internal rod pressure exceeding system pressure. For intermediate and full power conditions, fuel cladding failure is presumed if local heat flux exceeds thermal design limits (e.g. DNBR and CPR).
2. The PCMI failure criteria is a change in radial average fuel enthalpy greater than the corrosion-dependent limit depicted in Figure 3.1-3 (PWR) and Figure 3.1-9 (BWR).

   The total number of fuel rods which must be considered in the radiological assessment is equal to the summation of all of the fuel rods failing each of the criteria. Applicants do not need to double count fuel rods which are predicted to fail more than one of the criteria.

Coolability Criteria:

1. Peak radial average fuel enthalpy must remain below 230 cal/g.
2. Peak fuel temperature must remain below incipient fuel melting conditions.
3. Mechanical energy generated as a result of (1) non-molten fuel-to-coolant interaction and (2) fuel rod burst must be addressed with respect to reactor pressure boundary, reactor internals, and fuel assembly structural integrity.
4. No loss of coolable geometry due to (1) fuel pellet and cladding fragmentation and dispersal and (2) fuel rod ballooning.

   Fuel rod thermal-mechanical calculations must be based upon design-specific information accounting for manufacturing tolerances and modeling uncertainties using NRC approved methods including burnup-enhanced effects on pellet power distribution, fuel thermal conductivity, and fuel melting temperature.

Fission-Product Inventory:

The total fission-product inventory available for release upon cladding failure equals the steady-state gap inventory (from the applicable RG) plus the transient release (calculated with the correlation provided in Section 3.3).

5.0 REFERENCES

1. P. E. MacDonald, S. L. Seiffert, Z. R. Martinson, R. K. McCardell, D. E. Owen, and S. K. Fukuda, "Assessment of Light-Water-Reactor Fuel Damade During a Reactivity-Initiated Accident," *Nuclear Safety*, Volume 21, 582, 1980.

2. NRC Memorandum, "Research Information Letter No. 0401, An Assessment of Postulated Reactivity-Initiated Accidents for Operating Reactors in the U.S.," March 31, 2004, ADAMS ML040920189.

3. EPRI Topical Report on Reactivity Initiated Accident: Bases for RIA Fuel Rod Failure and Core Coolability Criteria, 1002865, April 2002.

4. R. Manzel and C. T. Walker, "EPMA and SEM of fuel samples from PWR rods with average burn-up of around 100 Mwd/kgHM," Journal of Nuclear Materials, 301, 170-182, 2002.

5. J. Kamimura, K. Ohira, K. Okubo, N. Itagaki, "High Burnup Fuel (Pellet Burnup 80 GWD/T) Bahaviour - Fission Gas Release, Pellet Swelling, Micro-Structure," Technical Paper, ANS/ENS LWR Fuel Performance Conference, October 2006.

6. T. Nakamura, T. Fuketa, T. Sugiyama, and H. Sasajima, "Failure Thresholds of High Burnup BWR Fuel Rods under RIA Conditions," Journal of Nuclear Science and Technology, Vol 41, pp 37-43, January 2004.

7. T. Nakamura, M. Yoshinaga, M. Takahashi, K. Okonogi, and K. Ishijima, Boiling Water Reactor Fuel Behavior Under Reactivity-Initiated-Accident Conditions at Burnup of 41 to 45 GWd/tonne U, Nuclear Technology Vol 129, pp 141-151, February 2000.

8. T. Nakamura, K. Kusagaya, T. Fuketa and H. Uetsuka, "High-Burnup BWR Fuel Behavior Under Simulated Reactivity-Initiated Accident Conditions," Nuclear Technology Vol. 138, pp 246-259, June 2002.

9. T. Fuketa, H. Sasajima, Y. Tsuchiuchi, Y. Mori, T, Nakamura, and K. Ishijima, "NSRR/RIA Experiments with High Burnup PWR Fuels, Proceedings of 1997 International Topical Meeting on Light Water Fuel Performance, Portland, Oregon, March 2-6, 1997.

10. T. Fuketa, T. Sugiyama, H. Sasajima and F. Nagase, "NSRR RIA-simulating Experiments on High Burnup LWR Fuels," Proceedings of the 2005 Water Reactor Fuel Performance Meeting, Kyoto, Japan, pp. 633-645, October 2-6, 2005.

11. F. Lemoine, J. Papin, J. Frizonnet, B. Cazalis, and H. Rigat, "The Role of Grain Boundary Fission Gases in High Burn-Up Fuel Under Reactivity Initiated Accident Conditions," Fission Gas Behavior in Water Reactor Fuels - Seminar Proceedings Cadarache France, 26-29 September 2000.

12. L. Yegorova et al, Experimental Study of Narrow Pulse Effects on the Behavior of High Burnup Fuel Rods with Zr-1%Nb Cladding and UO_2 Fuel (VVER Type) under Reactivity-Initiated Accident Conditions: Program Approach and Analysis of Results," NUREG/IA-0213, Vol. 1, May 2006.